



A minireview on Applications of the Metal-Organic Framework and Carbon Dots in Dye Photodegradation to Protect the Aquatic Environment from Organic Pollutants



A. A. Abd El Khalk ^{a*}, M. A. Betiha ^{b*}, A. S. Mansour ^c, M. G. Abd El Wahed ^a, A. M. Al-Sabagh ^b

^a Chemistry Department, Faculty of Science, Zagazig University, Zagazig, Egypt.

^b Egyptian Petroleum Research Institute, Cairo, Egypt

^c National Institute of Laser Enhanced Sciences (NILES), Cairo University, Egypt

Abstract

Water is the cornerstone of all life. With cascading warnings of water shortages, treating wastewater to achieve the purity required for various applications ranging from irrigation of crops to its use in drinking water is critical. Both carbon dots and MOFs have attracted intense interest, and many investigations have been raised, especially concerning their function as photocatalysts. The carbon dots show great advantages: biocompatibility, ease of conducting chemical reactions to change the nature of their surface, good colloidal stability, and low cost. These good qualities give both carbon dots and organic metal frames great potential to replace the traditional catalysts currently used in treating water from organic dyes. The applications of metal-organic frameworks (MOFs), which contain photo-active sites, especially ZIF-8, in the field of photocatalysis to remove dyes as water pollutants, have been discussed. The MOFs materials prepared by bonding metal ions with the organic ligands showed superior photoactivity properties to their individual counters. This article summarizes the progress made in preparing carbon dots and summarizing the synthesis methods and emission mechanisms. We envision that the carbon dots will ultimately have significant commercial use and become a strong competitor to some fluorescent materials currently used to treat wastewater. This review provides insights into both basic research and practical applications of carbon dots.

Keywords: MOFs; Carbon dots; Photodegradation; water pollutants; organic dyes

1. Introduction

Water, for all living things on Earth, is the basis of life. Confronting limited water resources with increasing urbanization requires highly advanced technologies to ensure water quality. Water is life as it directly affects human health. Likewise, many industries and economies depend on freshwater [1]. The percentage of farm water directed to irrigation of crops represents about 40% of the farm water, and 20-40 liters per person consumes the interface in its daily use and may increase to 50 liters per day according to the place in which the person resides. Consequently, the human race's consumed water, whether for personal use or in industry, represents a huge proportion that must be utilized by disposing of industrial or household wastes [2]. According to the World Health Organization, water pollution has been defined as bacterial, chemical, physical, or radioactive contamination or any additives that may affect water's

physical properties [3]. Water pollution has many negative effects on the living, human beings, the environment, and aquatic communities. Water pollution causes approximately 14,000 deaths per day, mostly due to contamination of drinking water by untreated sewage in developing countries [4]. Generally, the pollutant comes from sewage, and industrial effluents discharged into the river without pretreatment and surface runoff from agricultural land where fertilizer, pesticides, insecticides, and manures are used [5].

Chemical pollutants of water, whether organic or inorganic, are the most dangerous to the ecosystem and represent a real threat in various countries. Industrial wastes contain many chemicals that are difficult to decompose environmentally [6]. Some industries tend to color their products, especially the products we deal with daily, to improve their vault and shopping attractiveness. Many chemical dyes are

*Corresponding author e-mail: amira.a.abdelkhalk1311@gmail.com (A. A. Abd Elkhalk); Mohamed_betiha@hotmail.com.

Received date: 16 April 2021; revised date: 27 May 2021; accepted date: 13 June 2021

DOI: 10.21608/EJCHEM.2021.72540.3602

©2021 National Information and Documentation Center (NIDOC)

widely used to enhance the shape of these products and are usually non-toxic. Still, some dyes are used industrially and effectively in large industries such as textiles, leather tanning, plastics, paper, and cosmetics that harm living organisms and even agricultural soil and groundwater [7].

Organic dyes are one of the main pollutants released into industrial wastewater from textile factories, especially organic dyes soluble or poorly soluble in water. Those classified internationally as reactive, direct, and basic/acidic. Since it has a high solubility in water, its removal by traditional methods is a challenge [8, 9], for example, but not limited to, the global production of color pigments is close to 800,000 tons per year, and about 10-15% of these dyes are lost during the textile dyeing process [10]. A large amount of potable water is wasted by the textile industry (i.e., about 200 liters of water is consumed to produce 1 kg of textiles), so a large amount of wastewater is usually discharged without taking into account any pretreatment, which leads to an increase in water pollution [11]. Dyes dissolved in the wastewater of textile factories cause great harm to aquatic organisms. It reduces and sometimes prevents sunlight permeability in the water, reducing the rate of photosynthesis in aquatic plants and causing a decrease in the level of dissolved oxygen [9]. Highly colored waste of industrial pollutants is considered the most dangerous and causes cancer, as it is directly related to the destruction of the environment and the emergence of multiple diseases for living organisms [12], so the formation of scientific research at their disposal has become an imposed matter [13]. In general, chemical, physical and biological treatment procedures can be used for this purpose; These procedures differ in their efficiency, whether in the dissolution of the dyes or their adsorption efficiency, cost, and yield [14].

There are many types of research, in addition to those concerned with water purification using nanomaterials, which are receiving high attention, especially in the field of energy such as hydrogen [15-17], biodiesel production [18-25], and also our groups have published the use of nanometric materials in the production of production and transportation of heavy oil [26-34] and others [35, 36] to secure the human race's needs of clean and renewable energy. Here, this review will discuss two nanocomposites, namely metal-organic framework and carbon dots, and their role in removing pollutants from water. Emphasis will be placed on the preparation methods, the morphology of the prepared compounds, and the results of their use as photocatalysts or adsorbents for toxic dyes removal from water. In addition, this review provides an objective, comprehensive overview through a

systematic discussion of methods for preparing MOFs and carbon dots and an in-depth look at the different preparation methods for these materials. Its performance is reviewed as photocatalysts by itself or loaded with some materials and a review of its mechanism of action.

2. Metal-organic framework

By seeking to find new porous materials that differ in their composition from zeolite compounds and their derivatives, it was found that Metal-organic frameworks (MOFs) are among the most important porous group members' materials [25, 37, 38]. MOFs are of unparalleled interest due to their large surface area compared to functionalized mesoporous materials [34, 39-49], polymer membrane [42, 50] and ease of surface grafting with various functional chemical groups, and large pore size. MOFs are aromatic or aliphatic moieties attached to carboxyl, amine, or imidazole groups with some transitional elements. MOFs have proven their distinction over others in many areas, including adsorption [51, 52], storage of various gases, separation of liquids and gases [53], and heterogeneous catalysis [51, 52, 54]. More specifically, MOFs are composed of mono-metallic ions or metallic clusters [55-58] coordinated 1,4-benzene dicarboxylic acid, 1,3,5-benzene tricarboxylic acid, 4,4'-bipyridine; 4,5-imidazole dicarboxylic acid, biphenyl-4,4'-dicarboxylic acid, 4-bis[(1H-pyrazole-4-yl)ethynyl]benzene, etc., [59] (**Figure 1**). Interesting features are that MOFs have distinct properties, for example, their crystallinity combined with extremely high porosity (up to 90% of the free volume), massive interior spaces extending beyond 6000 m²g⁻¹, and a well-defined crystalline structure, which increases their applications [60-64].

For the first time, MOFs with considerable porosity were prepared in 1995 by the scientist Yaghi and Li [65], who used 4,4'-bipyridine as a linker and Cu(I) as a central metal. The authors found that the obtained material had a three-dimensional crystalline framework containing pore space with a channel ($\approx 2 \times 4 \text{ \AA}$). These channels are similar to some zeolitic types, such as analcime and natrolite. They also found that this substance has good stability in the air for long periods, while its stability in boiling water reaches one hour.

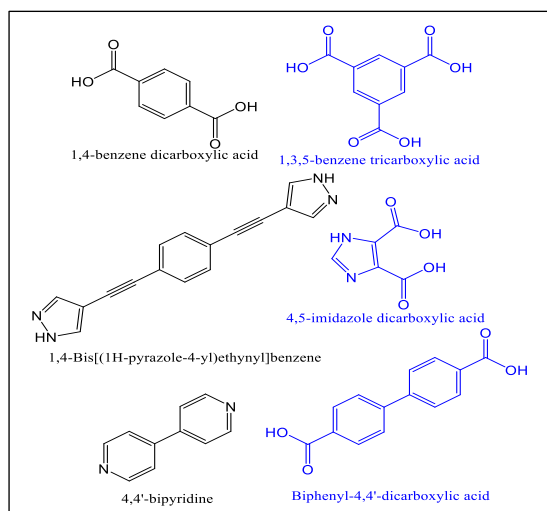


Figure 1. Some examples of MOFs's legends [59, 66].

There are over 70 000 MOFs recorded in the Cambridge Structural Database [67]. The material of Institut Lavoisier is known as MIL MOFs (MIL-53, MIL-100, and MIL-101), which are composed of inorganic moieties (lanthanide or transition metals) and legends (terephthalic or trimesic acid) [68]. The University of Oslo series, known as UiO-66 and UiO-67 MOFs, comprises zirconium oxide as transition metal coordinated 1,4-benzene dicarboxylic acid or biphenyl-4,4'-dicarboxylate as ligands [69]. Hong Kong University of Science and Technology fabricated HKUST-1 from Copper nitrate trihydrate and 1,3,5-benzene tricarboxylic acid in basic conditions [70]. IRMOF series is the largest series where the zinc nitrate could be replaced by different metals to coordinate terephthalate ions, and also the other ligands could be introduced [71]. Zeolitic-MOFs series (ZIF-8, ZIF-10, ZIF-68, and ZIF-69) were fabricated from different imidazole moieties as ligand and a zinc-metal [72].

ZIFs are a class of imidazole zeolite frameworks with three-dimensional porous structures that arise from imidazole derivatives' interaction with the tetrahedral metal ions, like zinc or cobalt. The fact that the angle between the metal-imidazole-metal corresponds to the angle of zeolites ($-\text{Si}-\text{O}-\text{Si}-$, 145°) has led to more interest in this class [1, 2]. ZIFs are characterized by ease of preparation, high porosity, and considerable thermal and chemical stability; these qualities make them candidates for adsorption and gas storage applications. Although ZIFs have a unique advantage over zeolites, the hybrid system frameworks of ZIFs are supposed to have more surface modification flexibility and often allow surface properties to be rationally built [73-75]. The ZIF-8 (**Figure 2**) framework ($\text{Zn}(\text{MeIM})_2$), one of representative

MOFs, was used as a support; it holds an intersecting three-dimensional structural feature, large pore size (diameter of 11.6 \AA), large surface area, and high thermal stability (over 500°C) [76].

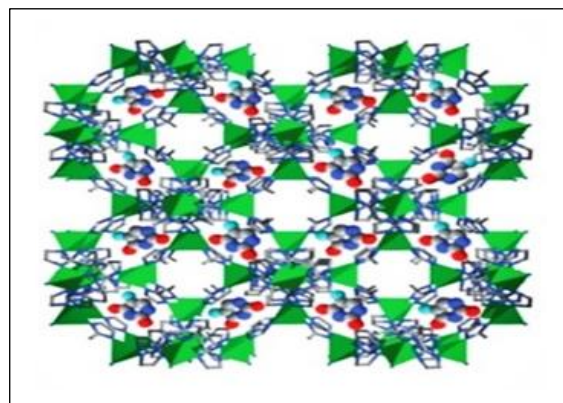


Figure 2. Graphic diagram presented two strategies of the summarized 5-Fu released from ZIF-8. C = grey, N = blue, O = red, F = light blue, Zn = green, [77].

3. Carbon Quantum dots

Due to quantum dots' advantages such as low cost, excellent sensitivity, fast response time, fluorescence (FL) based sensing, quantum dots have attracted a lot of attention [78]. Carbon materials and their derivatives always find their way to be in the focus of scientists' interest, as they can be found in many configurations with unique chemical and physical properties such as diamond, nano-diamond graphite, activated carbon, charcoal, carbon nanotubes, fullerene, and more recently, graphene and quantum dots (CQDs). Quantum dots (QDs) are semiconductor nanocrystals with dimensions smaller than the exciton Bohr radius, and carbon dots (CDs) generally refer to small carbon nanoparticles, in a broad definition of aqueous or other suspensions. CDs are new forms of discovered fluorescent nanomaterials that have emerged to be extremely common in the last decade due to their unusual optical properties, low toxicity, biocompatibility, high aqueous stability, rapid synthesis, etc. [78-80] (**Figure 3**).

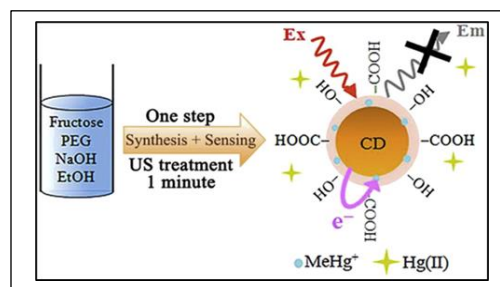


Figure 3. Preparation of fluorescent carbon dots and the sensing of methylmercury [81].

The CQDs were discovered by accident during the separation and purification of single-walled carbon nanotubes (SWCNTs) by Xu et al. in 2004 [82]. That caused the following surveys to utilize CQDs' optical properties and generate a new category of applicable fluorescent nanomaterials. Fluorescent carbon nanomaterial was termed "carbon quantum dots" by Sun in 2006, who submitted a synthesis technique via surface passivation to generate CQDs with higher fluorescence emissions [83]. The top-down method [82-84] and the bottom-up methods were used to synthesize CQDs [85-87] (**Figure 4**).

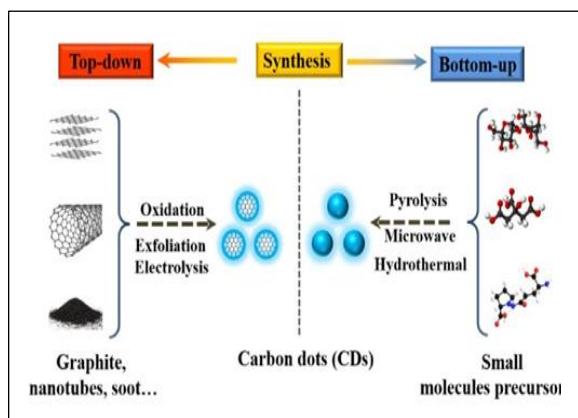


Figure 4. Different approaches of CD synthesis [88].

3.1. Top-down approaches for fabricating carbon dots

3.1.1. Arc-discharge method

Xu *et al.* [82] note that by using the electrophoresis method (using an electric current to move particles inside a porous gel, where the function of the pores in the gel is to sift these particles to allow the smaller ones to pass more quickly than the rest of the particles) to purify single wall-carbon nanotube soot. The authors notice a faster-moving layer than long nanotubes and shorter tube materials, and they named it nanodots. The nanodots were distinguished by light emission when they were excited at 365 nm, and elution light emission could be separated into four bands (green, blue, yellow, and orange) (**Figure 5**). The nominal molecular weight limit (NMWL) was 3–10 K, 10–30 K, 30–50 K NMWL, and their composition was 55.93%-carbon, 2.65%-hydrogen, 1.2%- nitrogen, and 40.33%-oxygen.

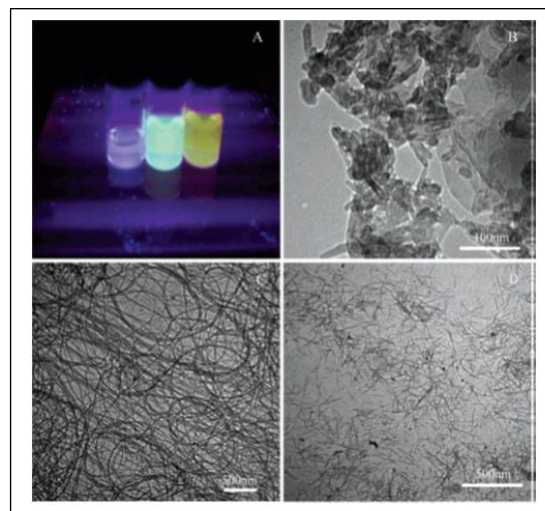


Figure 5. (A) Fractions of fluorescent carbon under 365 nm, (B) TEM tubule carbon, (C) purified SWCNTs, and (D) chopped SWCNTs [80].

3.1.2. Laser ablation/irradiation approach

Sun *et al.* [89] proposed a new approach for preparing carbon-based fluorescent nanomaterials and labeling them with carbon dots. Carbon dots were obtained by laser ablation of a carbon target in the presence of inert gas (argon) and water vapor as carriers. The graphite powder and cement were hot-pressed to obtain the carbon target, then a gradual treatment of baking and annealing under an argon flow was performed. The resulting carbon sample was refluxed in 2.6 M nitric acid for 12 h. The surface passivation of the carbon sample with poly(ethylene glycol) diamine compound ($\text{H}_2\text{N}(\text{CH}_2\text{CH}_2\text{O})_n\text{CH}_2\text{CH}_2\text{NH}_2$, $n \sim 35$) resulted in photoluminescence. This was followed by the reporting of other techniques, including the combination of laser ablation and simultaneous surface passivation processes (a single process) [90-92]. Pulsed Nd: YAG laser was used to irradiate graphite-organic solvents, achieving the simultaneous synthesis of surface passivated carbon dots. The researchers also suggested that the emission properties of carbon dots can be adjusted by properly selecting the organic solvent, such as different molecular weight poly(ethylene glycol) diamine, diethanolamine, etc. [93].

3.1.3. Electrochemical approach

For the first time, Ding and coworkers introduced a new approach to preparing carbon blue dots from multi-walled carbon nanotubes using an electrochemical approach [94]. MWCNTs were prepared by a chemical vapor deposition method, and CDs were designed in a mixture of acetonitrile and

tetra-ammonium perchlorate as the supporting electrolyte solution. After a certain number of cycles, the mixture solution turned dark brown due to carbon dots' formation. The purified CDs' size was 2.8 nm with a lattice spacing of 3.3, characterized by emitting bright blue light when excited by a 340 nm light source. Li et al. [95] also use an electrochemical approach to obtain carbon dots using anode and cathode made of graphite. The authors note that carbon dots are successfully formed in the basic electrolyte (NaOH/EtOH) and cannot be obtained in an acidic electrolyte (H₂SO₄/EtOH) (Figure 6). Carbon dots have a diameter of less than 4 nm with a lattice spacing of about 0.32 nm. Similarly, carbon dots can be obtained from graphene films and carbon fibers [95-97].

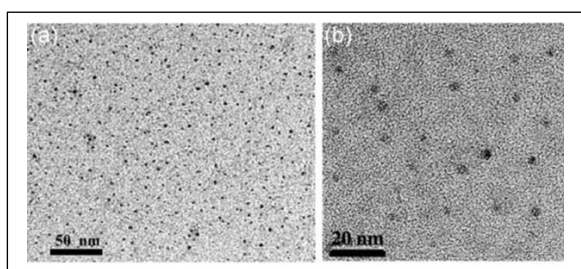


Figure 6 (a,b). TEM images of as-prepared GQDs [95].

3.1.4. Chemical exfoliation method

Liu et al. [98] report on preparing, purifying, and characterize fluorescent, multicolored carbon nanoparticles with a size less than 2 nm. The carbon nanoparticles were prepared from the combustion candle soot's oxidation (using 5 M HNO₃) as a common carbon resource. Polyacrylamide gel electrophoresis was utilized to purify and separate the particle size of the resultant carbon material. The resulting material was fluorescent by excitation with ultraviolet rays of a single wavelength (312 nm). Peng et al. [99] prepared graphene quantum dots, GQDs, with great optical and electronic properties. The quantum dots are fabricated from the chemical exfoliation (using a mixture of H₂SO₄ and HNO₃) of cheap and commercially available material, pitch-based carbon fibers (Figure 7). The as-produced GQDs had a 2D zigzag edge morphology with a narrow size of 1-4 nm. by changing process parameters, the PL of the GQDs can be detailed by resizing the GQDs. Ye et al. [100] have reported an easy approach to assemble tunable GQDs from different types of coals. It has been demonstrated that the unique coal structure has been shown to have the unique advantage of producing GQDs over other sp²-carbon allotropes. Oxidation makes it easier to displace the crystalline carbon within the coal

structure than the pure sp²-carbon structures, resulting in nanometer-sized quantum dots with amorphous carbon available at the edges (Figure 8).

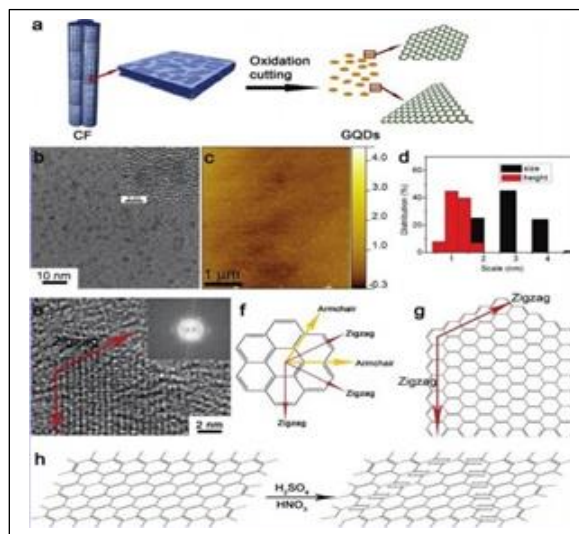


Figure 7. (a) Oxidation cutting scheme of CF to GQDs. (a) (b) the GQD's TEM photos (synthesised temperature of the reaction at 120 °C) and (b) the GQD's HRTEM. (c) GQD AFM photo. (d) GQDs distribution of size and height. (e) GQD Edge HRTEM graphic, 2D FFT Edge in inset in (e). (f) Schematic diagram illustrating the alignment and the relatively zigzag and armchair paths of the hexagonal graph network. (g) Schematic diagram of the HRTEM image edge termination in (e). (h) Described GQD chemical oxidation process for CF [99].

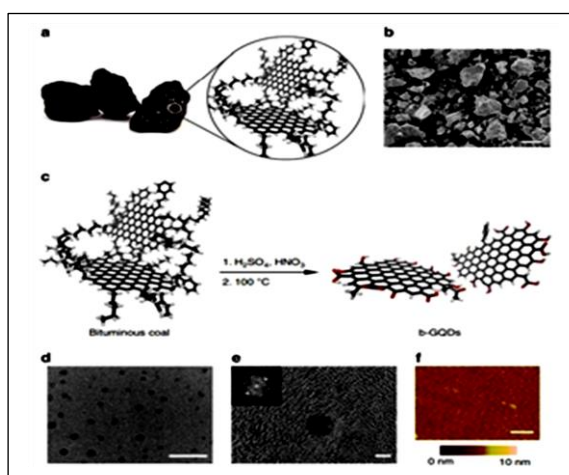


Figure 8. (a) Simplified macro image. (b) SEM representation of coal (c) The b-GQD synthesis schematic illustration. (d) B-GQDs TEM (e) the HRTEM image of b-GQDs representative. (f) b-GQD b-AFM [100].

3.2. Bottom-up approaches for fabricating carbon dots

3.2.1 Thermal pyrolysis approach

Giannelis et al. [101] documented the pyrolysis method for producing nano-carbon materials. The authors used ammonium citrate as a carbon source to fabricate carbon dots, while the ammonium counterpart was a modifier. The physical properties of the carbon surface's nature, whether hydrophilic or hydrophobic, can be controlled by changing the carbon source. For example, octadecyl ammonium citrate ($C_{60}H_{125}N_3O_7$) was used to produce a hydrophobic surface nature, and 2-(2-aminoethoxy) ethanol ($C_4H_{11}NO_2$) used to denature the surface of a hydrophilic. In both types, the ammonium carboxylate thermal dehydration leads to the formation of covalent amide bonds, taking into account the different sample preparation pathways. Organophilic surface carbon dots fabricated from ramping calcination of carbon source (e.g., citric acid) in the air (300 °C), while hydrophilic carbon dots fabricated from the hydrothermal of a mixture of citric acid and 2-(2-aminoethoxy) ethanol. The organophilic carbon dots showed a sharp monodispersed size of 7 nm than the hydrophilic carbon dots. The effect of temperature change on carbon points' nature resulting from the pyrolysis process citric acid and citric acid – ethanolamine was studied by Giannelis et al. [102].

The authors showed that pyrolysis at 180 °C for half an hour leads to carbon dots' production, whose particles cannot be observed by DLS or TEM analyses. They have a strong excitation-independent PL emission arising from organic fluorophores. More specifically, the amide bonds contributed to the emission of carbon dots. With an increase in temperature to 230 °C, spherical carbon dots of 19 nm in size were formed to be observed with TEM. The authors explained that the temperature increased the entanglement between the carbon dots formed by increasing the synthesis of covalent amide bonds. Increasing the temperature to 300 °C led to the formation of carbon dots with an average size of 8 nm. The small size of the carbon dots, in this case, is produced from the emission of carbon dioxide during the pyrolysis process. Irregular particles of carbon dots appeared by increasing the degree of the pyrolysis process to 400 °C due to the aggregation of carbon dots; however, these carbon dots retained their optical properties. Wang et al. [103] have documented an easy chemical method for synthesizing highly efficient carbon dots by surface passivation of crude carbon dots (CDs) with poly(ethylene glycol) that, when irradiating with 407 nanometers-light, emit white light from solution and film. The carbon dots are synthesizing through the thermal oxidation in molten

lithium nitrate under inert gas. The choice of nitrate counter anion is due to nitrate's ability to serve as oxidizing media, forming O^{2-} or O. The carbon dots are well-dispersed in different solvents and had stable PL at different pH values. The surface passivation carbon dots with poly (ethylene glycol) showed a broad visible spectrum emission when excited with blue light (**Figure 9**). Guo et al. [104] prepared carbon dots from unzipping of as-prepared epoxy-enriched surface polystyrene colloidal crystal with the desired size through the calcination process (200, 300, and 400 °C for 2 h under inert gas). Upon UV-irradiation, the carbon dots calcined at 200 °C showed bright blue fluorescence while calcined at 300 and 400 °C showed orange and white fluorescence (**Figure 9**). Liu et al. [105] used a green route to fabricate fluorescent carbon dots using a one-step pyrolysis process of hair as a new precursor of carbon dots. This strategy was characterized by using non-toxic solvents or expensive raw materials and providing an effective way to take advantage of the hair waste. The as-prepared carbon dots showed high compatibility with hydrophobic polymer (poly (methyl methacrylate)) and hydrophilic polymer (polyvinylpyrrolidone) that exhibit blue fluorescence when irradiated with UV-light.

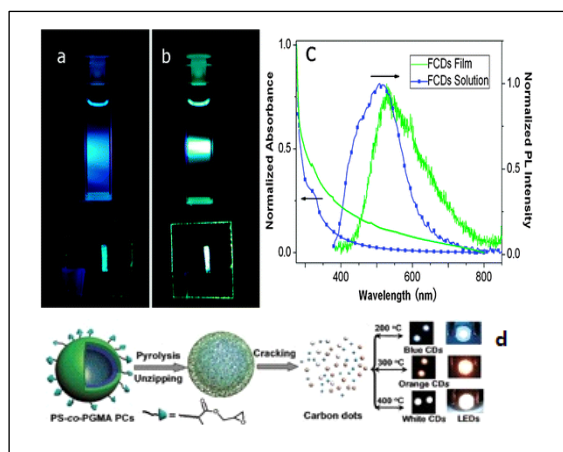


Figure 9. Optical photograph of the FCDs solution and film excited by (a) 5 mm commercial UV LED (375 nm), (b) 407 nm laser and (c) corresponding absorption and emission spectra of the FCDs solution and film excited at 407 nm [103], (d) Schematic illustration of the pyrolysis of photonic crystals production of carbon dots [104].

3.2.2. Hydrothermal method

The hydrothermal method's manufacture of carbon dots was reported in 2011 [106] by dissolving monopotassium phosphate and glucose at specific molar ratios in water. Next, the mixture was transferred, after deoxygenation, to a Teflon-lined

autoclave and heated at 200 °C for half a day. After separating the sediment using centrifugation, the upper layer was freeze-dried and re-dispersed with ethanol to form a suspension. The advantage of this approach from others is that the formation of carbon points and their surface treatment occur simultaneously. The variation of glucose/to KH_2PO_4 molar ratio resulted in turning the PL properties; for example, when carbon dots resulted from glucose:26- KH_2PO_4 excited by UV-irradiation, the carbon dots showed green emission. In addition to glucose, other natural resources could be used to manufacture carbon dots at low temperatures (150 °C), such as orange juice. The authors suggested that the carbon dots resulted from the hydrothermal carbonization of the orange juice's organic components. Carbon dots were rich in -OH and -COOH function groups, giving carbon dots excellent water solubility [107] (**Figure 10**). The carbon dots were spherical with a diameter ranging from 1.5 and 4.5 nm. This strategy has resulted in further work on biotic resource modules for carbon dots synthesis [108].

Hsua and Chang [109] proved that carbon dots with hydrophilic surface nature and photo-active properties could be prepared from different organic compounds containing carboxyl and amine groups. The authors used glycine, 2-amino-2-hydroxymethyl-propane-1,3-diol, cadaverine ($\text{NH}_2(\text{CH}_2)_5\text{NH}_2$), and ethylenediaminetetraacetic acid by one-pot hydrothermal synthesis at 300 °C for 2 h. The authors suggested the carbon dots prepared through multi-steps, including water elimination, enable polymerization, carbonization, and surface passivation. The carbon dots morphology was spherical (2.6 ± 0.5 , glycine; 3.3 ± 0.4 , 2-amino-2-hydroxymethyl-propane-1,3-diol; 3.0 ± 0.5 , ethylenediaminetetraacetic acid; and 7.9 ± 0.8 nm, cadaverine, with a lattice spacing distance of 3.4 Å. All carbon dots showed blue PL as excited by 365 nm light. By selecting the appropriate organic molecules and controlling the reaction conditions of pH, temperature, and molar concentration, it is possible to obtain carbon dots covering the visible range [110-112].

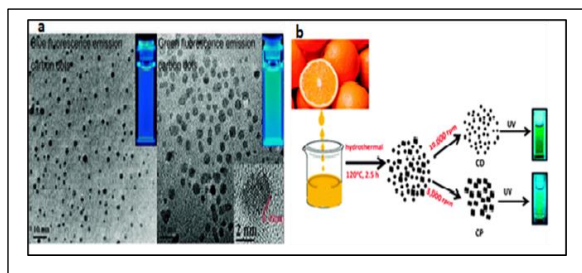


Figure 10. (a) TEM images of C-Blue and C-Green [106], (b) Illustration of formation of CDs from hydrothermal treatment of orange juice [107].

3.2.3 Microwave heating method

Zhu et al. [113] first discovered the method of microwave pyrolysis to prepare carbon dots. They considered this method comfortable and clean, and the possibility of using it on an industrial scale is great. The authors have used poly (ethylene glycol) (Mn 200) and polysaccharides such as glucose as feedstock. The ingredients were dissolved in water and heated in a microwave oven (500 watts) for a period of 2-10 minutes. It was observed that at the end of the reaction, the color of the mixture changed from transparent to dark brown, expressing the formation of carbon dots (**Figure11**). The resulting carbon dots were well dispersed in water, as XPS analysis showed that they are rich in different oxygen groups (hydroxyl and carbonyl), which are expected to have application in biotechnology. The resulting carbon dots were characterized by a size proportional to the reaction time, meaning that it was easy to control the resulting size of carbon dots, for example, heating for 5 minutes resulted in a volume of 2.57 ± 0.45 nm, while heating for 10 minutes produced a size of 3.65 ± 0.6 nm. Zhai et al. [114] made carbon dots, which have low cytotoxicity, by microwave-assisted pyrolysis of citric acid in the presence of different amine molecules (1,2-ethylenediamine), as the passivation agents. Upon excitation, the 1,2-ethylenediamine-carbon dots (EDA-CDs) at 300 nm, a bright blue PL-emission observed at 460 nm. The EDA-CDs have shown high dispersibility in water and had a particle size of 2.2-3 nm (**Figure12**). Chandra et al. [115] used a one-step to manufacture highly fluorescent crystalline carbon nanoparticles by microwave-irradiating sucrose and phosphoric acid solution at 100 watts for 3 minutes 40 seconds. The authors consider this method to be very simple, fast, and economical, and it can be used for industrial preparation to manufacture fluorescent crystalline carbon nanoparticles. The carbon nanoparticles (3-10 nm) emit bright green fluorescence under UV-light irradiation and can be used in bioimaging and drug delivery. The authors increased the fluorescence property of carbon nanoparticles by the addition of dyes (rhodamine B and α -naphthylamine). Dyed-carbon showed a maximum fluorescence intensity at an excitation wavelength of 225 nm, and at any other excitation wavelength, the peak positions were exactly the same as those of the carbon nanoparticles themselves. Likewise, Qu et al. [116] have reported the synthesis of water-soluble green luminescent carbon dots from citric acid and urea in a simple and low-cost microwave one-step method and their application as a new bio-compatible fluorescent ink. The most important characteristic of these carbon dots is that they are zero-toxicity to plants and animals. Sun et al. obtained red emissive ($\lambda_{\text{max}} \approx 640$ nm) and low

cytotoxicity carbon dots prepared by microwave approach. The carbon dots showed 43.9 % photothermal conversion upon laser irradiation (631 nm).

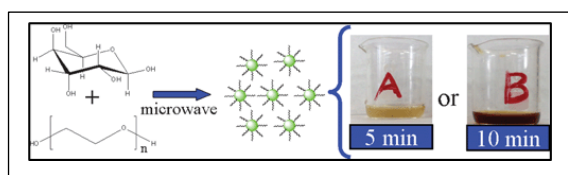


Figure 11. Microwave pyrolysis approach to CNPs [113]

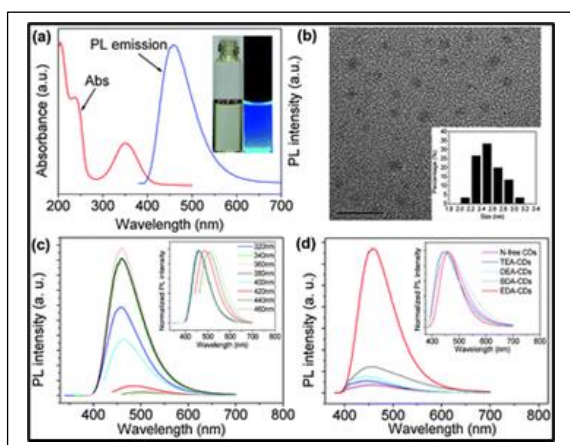


Figure 12. (a) UV-Vis and PL emission spectra of the CDs aqueous solution ($\lambda_{\text{ex}} = 360$ nm). (b) HRTEM graphic of CDs with a scale bar of 10 nm. (c) CD photoluminescence emission spectra (the inset is the normalised PL emission spectra). (d) PL spectra of CDs produced by various amine molecules (excited at 360 nm) (the inset is the normalised PL spectra) [114].

3.2.4 Anchor/support-based approach

Liu et al. [117] developed a chemical synthesis method that was easy to manufacture multi-colored photoluminescent amorphous carbon dots. Carbon dots with sizes ranging from 1.5–2.5 nm in diameter were obtained using silica colloidal modified with surfactant (triblock copolymer, F127), which was considered as a binder that locates between the silica spherand the carbon feedstock (resols, phenol-formaldehyde resin). The F127-polymer has been found to be the critical factor in the formation of the satellite-like composite. The resulting carbon dots have a tiny size (1.5–2.5 nm), and acid treatment and surface passivation are critical to achieving water-soluble and multicolor photoluminescent carbon dots (**Figure 13**). Wang et al. [118] reported the preparation of carbon dots from N-methyl piperidine occluded in a CHA zeolite with different luminescence; cyan,

blue, and green luminescent be separated from the as-prepared as prepared carbon dots. Bourlinos et al. [119] fabricated carbon dots using the 2,4-diaminophenol dihydrochloride exchanged cations in NaY zeolite. The carbon dots emission shifts to longer wavelengths as the visible excitation wavelength increases.

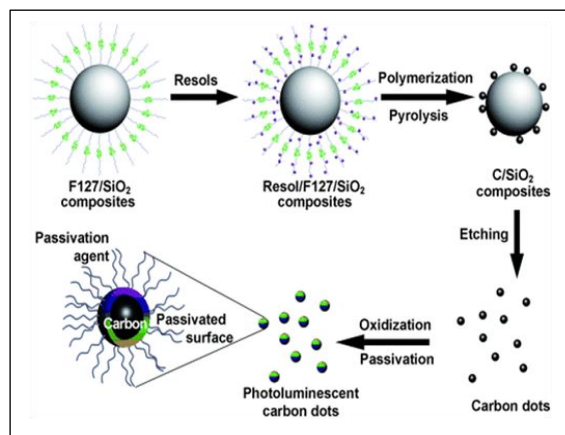


Figure 13. Assembly diagram for multicolored carbon dot synthesis [117].

Most of the applications that had been tested or suggested for CQDs depended on the photoluminescence of CQDs, such as bioimaging application, disease detection, and drug delivery [79, 120, 121], disease detection, and drug delivery [122]. And the susceptibility of the Photoluminescence of CQDs to the external environment allows them to be used as passive or active Nanosensors. Moreover, CQDs are used to detect metal ions, Organic compounds, inorganic compounds, and visualization [123]. Carbon dots are used for self-targeted bioimaging and diagnosis of tumor cells and tumor theragnostic [121, 124, 125].

3.2.5 MOF template-based approach

To obtain carbon dots of very small size, MOF compounds with small pores with a pore size of 1–2 nm can be used as a template for preparing carbon dots. Gu et al. [126] used HKUST-1 MOF loaded with glucose to synthesize photoluminescent carbon dots. The MOF was soaked with a mixture of glucose and ethanol (1:9) followed by very gentle evaporation of ethanol, and the weight difference MOF weight confirmed the success of filling the MOF pore with glucose, where it became 1.3 g. By heating the glucose-laden MOF at 200 °C (below the temperature needed to break down the MOF structure), glucose begins to decompose. The authors noticed a change in the color of the MOF material from blue to green, which the authors considered the change as evidence

of the formation of carbon dots. To reinforce this idea, the authors measured the nitrogen adsorbed of MOF before and after calcination, as the ability of the substance towards nitrogen adsorption decreased from 130 to 5 $\text{cm}^3 \text{g}^{-1}$. To release the carbon points formed from MOF pores using a potassium hydroxide solution (Figure 14). The purified carbon dots showed an average diameter of 1.5 nm, matching the diameter of the HKUST-1 pores. The researchers attributed this behavior to the nucleation of the carbon feedstock in the larger pores. Different sizes of carbon dots are produced by choosing the pore sizes of other MOF materials. For example, ZIF-8 and MIL-101 were used to produce carbon dots with 2.0 and 3.4 nm sizes, respectively. The carbon dots showed red-shift photoluminescence as the particle size of the carbon dots increases when excited by UV light

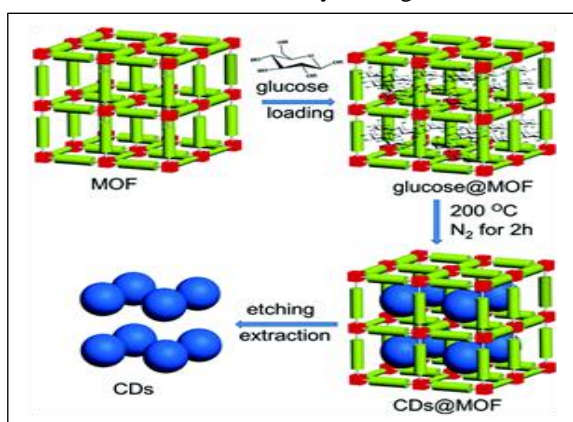


Figure 14. Mechanism of preparation carbon dots prepared using MOF as templates [126, 127].

Xu et al. [128] achieved carbon dots using MOF (0.25 g of ZIF-8C) as a starting material loaded on the porous silica griddle of a glass steamer. The material is transferred to an autoclave filled with 2 ml nitric acid. The autoclave was heated to 160 °C for 5 h. The produced nitrogen-doped carbon dots were separated from a glass steamer in water and harvested by filtration. The formed carbon dots' size distribution was narrow (1.3-2.7 nm) with an average diameter of 2 nm and crystalline. (Figure 15). The nitrogen-doped carbon dots successes as a selective fluorescent probe for the ferric detection

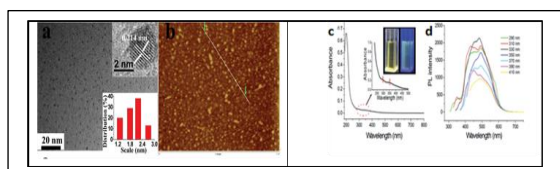


Figure 15. (a, b) A typical TEM image of the N-GQDs.; (c) UV-vis of the N-GQDs. (d) PL of the N-GQD at different excitation wavelengths from 290 to 410 nm. [128].

Yang et al. [129] used mesoporous silica (Santa Barbara, SBA-15) as a template for synthesizing photoluminescent carbon dots (soft-hard template approach). The carbon dots sources were 1,3,5-trimethylbenzene, diaminebenzene, pyrene and phenanthroline. The average carbon dots diameter was nm.

4. The removal of dye pollutants from the aqueous system.

Different treatment processes, such as oxidation, coagulation, filtration, ozonation, membrane filtration, reverse osmosis, ion exchange, electrochemical degradation, adsorption, and photodegradation, are used to remove dyes, especially MB, from wastewater [130-137].

4.1. photocatalysis

Photocatalysis is a phenomenon dating back nearly 200 years, and it can be described as an advanced oxidation process in the presence of a catalyst whose activity depends on the formation of pairs of electronic holes, which in turn generate free radicals such as hydroxyls that are able to undergo other secondary reactions [138, 139]. Due to the abundance of solar light (as an inexpensive energy source and light source), semiconductor-based heterogeneous photocatalysis is one technique that received extraordinary attention in recent times. Photocatalysis has focused on solving environmental pollution problems, which has become one of the most important global issues of concern to governments and their people. The photocatalysis concept was attributed to Edmund Becquerel in 1839 [140, 141]; however, this research did not receive appropriate attention until the late 1960s. Thanks to our pioneers in this field, Budi [142], Honda, and Fujishima [143], who have enriched this branch of science.

The concept of photocatalysis has also been used in the literature for two completely different processes [144]. Strictly speaking, the driving thermodynamically uphill reaction ($\Delta G > 0$) using a material activated by light energy is called photosynthesis. A material used in such a case can be considered a "photocatalyst" only if the photon is considered to be a reactant. An example of these states is chemical transformation, water splitting, and carbon dioxide reduction [145, 146]. Conversely, some materials may use light energy to easier thermodynamic downhill reactions ($\Delta G < 0$). In this case, the material is only changing the reaction's kinetics and does not change the thermodynamics of the reaction, and it is called a photocatalyst. For example, phenol oxidation ($\Delta G^\circ = -167.96 \text{ kJ/mol}$) [147]. The IUPAC definition of photocatalyst is a "catalyst able to produce, upon absorption of light, chemical transformations of the reaction partners. The photocatalyst's excited state

repeatedly interacts with the reaction partners forming reaction intermediates and regenerates itself after each cycle of such interactions [148].

Photocatalysts can be divided into six general categories, including (a) molecular photocatalysts (in this class of photocatalysts, the molecular orbital theory would be best suited to describe the system), Where the alignment of HOMO (highest occupied molecular orbitals) or LUMO (lowest occupied molecular orbitals) of the catalyst with the reactants molecular orbitals is more relevant; (B) Conventional semiconductor photocatalysts (the band theory is most suitable to describe the system); (c) quantum point photocatalysts (the optical and electrical behavior of a catalyst is sensitive to the size of the catalyst); (d) two-dimensional photocatalysts, and (f) semiconductor photocatalysts.

Several semiconductor photocatalysts (e.g., metal oxides, chalcogenides, and metal salts and their composites) have been developed for dye degradation. Still, photo corrosion, which is related to the oxidation of sulfide ions by photogenerated holes, often results in secondary contamination of heavy metal ions [149]. MOFs also have conduction and valence bands identical to semiconductors, relating to the center metal's empty outer orbitals and the organic component's outer orbitals, respectively [150, 151]. Compared to regular inorganic photocatalysts, photo-sensitive MOFs' light absorption ability is more adjustable due to the wide variety of organic linkers and metal centers during the construction of MOF structures and functionality.

MOFs are classified as semiconductors based on their optical transitions and their electrochemical, chemical, and photoelectric activities. Yet, these activities do not necessarily imply that it is a semiconductor material. Semiconductors have a delocalized valence and conduction bands range within which the charge carriers are mobile. Organic semiconductors typically have delocalized orbitals (conjugate bonds), facilitating charge carrier mobility. MOFs' degradation of organic contaminants during photocatalysis processes should be viewed as MOF is assembled molecular catalysts rather than conventional semiconductors. Consequently, photocatalytic pathways can be described by the term HOMO-LUMO gap [152].

Organic linkers (ligands) in MOFs can be thought of as light-harvesting units, as they transfer the energy of excited states to inorganic metallic clusters consisting of a few metal atoms. The photogenerated electrons will then be migrated from the highest occupied molecular orbital (HOMO) to the lowest unoccupied molecular orbital (LUMO) of the MOFs and then transferred to the metal-oxo cluster surface

(known as the Ligand-to-Metal Charge Transfer (LMCT) mechanism) [153]. In addition to the most widely employed LMCT mechanism, ligand-to-ligand transfer, metal-to-ligand transfer, and metal-to-metal-to-ligand transfer mechanisms have also been used to explain various photocatalytic mechanisms [154]. The metal-based MOFs can also be directly photo-excited to create electrons and holes [155]. Oxygen molecules will then absorb electrons generated by photo (e^-) to form superoxide radicals ($\cdot O-O^-$). Photo-generated (h^+) in the HOMO orbital could immediately oxidize organic molecules due to their strong oxidizing capability and can also react with water molecules to form hydroxyl radicals ($\cdot OH$) [156].

4.1.1. CQDs as photocatalyst:

Lu et al. [157] synthesized photocatalytic $ZnFe_2O_4/TiO_2/CDs$ nanocomposite hydrothermally, the photocatalytic activity under solar-spectrum irradiation of photocatalyst enhanced when a low content of CDs 3 wt % used where the CDs can efficiently develop the ability of electron transfer and separate the electron-hole pairs. Radical $\cdot OH$ and $\cdot O_2$ radical were confirmed to be involved in the photocatalytic degradation of RhB.

Zhang et al. [158] investigate the simple fabrication of Ag_3PO_4 , CQDs/ Ag_3PO_4 , Ag/Ag_3PO_4 , and CQDs/ Ag/Ag_3PO_4 photocatalysts., The photocatalysts complexes, CQDs/ Ag_3PO_4 and CQDs/ Ag/Ag_3PO_4 exhibit enhanced photocatalytic behavior and structural stability over the photodecomposition of organic compounds (methyl orange) under visible light irradiation due to the insoluble, photoinduced electron transfer, upconversion luminescence, and electron reservoir properties of CQDs. Furthermore, the catalytic performance of CQDs/ Ag/Ag_3PO_4 is the highest among Ag_3PO_4 and the related complex photocatalysts due to the synergistic effect of CQDs and the intense surface plasmon resonance of Ag.

Zhang et al. [159] prepared N-doped carbon quantum dots/ TiO_2 (NCQDs/ TiO_2) hybrid composites by using a low-temperature technique and photocatalytic behavior of the NCQDs/ TiO_2 hybrid composites was investigated using methylene blue (MB). The photodegradation efficiency of MB over 1NCQDs/ TiO_2 hybrid composites was 86.9% within 420 minutes, which was significantly higher than that of pristine TiO_2 (53.8%). The 10 NCQDs/ TiO_2 hybrid composites had the lowest photodegradation rate (49.3% removal efficiency), indicating that the excessive NCQDs minimize MB adsorption on the TiO_2 surface. The MB dye molecules were stimulated to create excited states (MB^*) as visible light was absorbed. The electrons in the MB^* can be excited to the conductive band (CB) of TiO_2 , transforming the

MB* into MB+•, which is needed for further photocatalytic reactions. The NCQDs facilitated electron transfer, resulting in effective electron -MB+• pair separation and improved photocatalytic activity, as showing in (Figure 16). The NCQDs' electrons could react with oxygen in the solution to create a radical. Oxygen. The radical ·O₂ produced would play an important role in the photodegradation process, resulting in dramatic photocatalytic efficiency. As a result, the work of NCQDs should be credited for the significantly improved visible photocatalytic performance of NCQDs/TiO₂, not only the sensitization effect of MB to TiO₂.

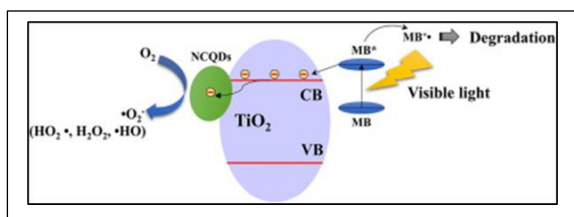


Figure 16. The important roles of NCQDs for enhancing the photocatalytic activity of TiO₂ with the separation and transfer of photogenerated charges in the NCQDs/TiO₂ hybrid composites under visible light irradiation [159].

Kannan et al. [160] Attempt to enhance the photocatalytic efficiency of cerium oxides (CeOx) by adding an in-situ produced heteroatom (-N and -S) doped carbon quantum dots/reduced graphene oxide (HDCQD@RGO) nanohybrid catalyst for organic pollutant degradation A simple, one-pot hydrothermal eco-friendly method was used to produce the CeOx-HDCQD@RGO nanohybrid catalyst (Figure 17). The HDCQD is essential for improving CeOx-RGO interaction and acting as a sensitizer for the electron-transfer process with CeOx. Multiple oxygen vacancies exist in the nanostructured CeOx, which assists in the generation of active oxygen and hydroxyl radicals. The photocatalytic method using nanostructured CeOx to generate active hydroxyl radicals results in improved organic pollutants photodegradation. Furthermore, the prepared CeOx-HDCQD@RGO nanohybrid catalyst has a better water oxidation reaction. The CeOx-HDCQD@RGO nanohybrid works well as a bifunctional catalyst in both energy and environmental applications. The process described by kannan et al. [160] is easy, environmentally sustainable, scalable synthesis of the highly effective catalyst.

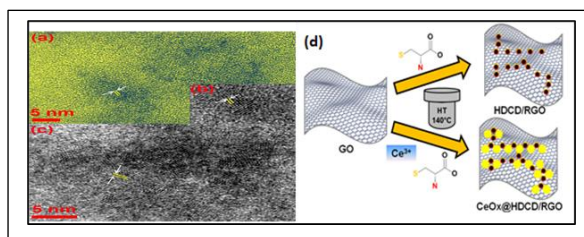


Figure 17. HRTEM micrographs of (a) HDCD@RGO and (b and c) CeOx-HDCD@RGO nanohybrid catalyst. (d) The synthesis process of CeOx-HDCD@RGO nanohybrid catalyst [160].

Atkin et al. [161] synthesized two-dimensional (2D) tungsten disulfide (WS₂) nanoflakes and hybridized them with carbon dots (CDs) using a simple two-step process that included exfoliation of bulk tungsten disulfide and microwave irradiation of nanoflakes in a citric acid solution. Compared to the pristine 2D WS₂, the hybrid content photodegraded roughly 30% more of the model organic dye in one hour.

Qu et al. [162] prepared (CQDs)/KNbO₃ composite successfully via hydrothermal and mixed-calcination methods. CQDs/KNbO₃ composites' photocatalytic behavior is evaluated via degradation of crystal violet dye as a target organic pollutant under visible-light irradiation. CQDs' presence as a co-catalyst on the surface of KNbO₃ particles is due to the creation of several more active sites for trapping electrons and facilitating the separation of photogenerated electron-hole pairs. Furthermore, CQDs can absorb visible light and emit ultraviolet lights to activate the wide band-gap KNbO₃.

ReddyPrasad et al. [163] prepared the Carbon dots (C-dots)/Copper tungstate (CuWO₄) heterostructure via a simple reflux method after synthesis of high fluorescent C-dots from dextrose via a simple ultrasonic wave supported reaction. Using rhodamine B as a model organic pollutant, the photocatalytic property of heterostructure nanocomposite was also examined. The photocatalytic activity of the heterostructure nanocomposite with 5.0 wt% C-dots is around three times that of pure CuWO₄.

Li et al. [164] used A basic one-step ultrasonic treatment to create a carbon quantum dots (CQDs)/Cu₂O composite with protruding nanostructures on the surface. The organic pollutant methylene blue was used to investigate the photocatalytic behavior of (CQDs)/Cu₂O under (N)IR light. The protruding nanostructures support different reflections of (N)IR light between the available space of these protruding particles, which can create excellent use of the source light and therefore deliver an enhanced photocatalytic activity, and CQDs can absorb (N)IR light (>700 nm), and then generate

shorter wavelength light (390–564 nm) as a result of up-conversion, which in turn motivates Cu_2O to form electron/hole (e^-/h^+) pairs (**Figure 18**). The adsorbed oxidants/reducers (usually O_2/OH) react with the electron/hole pairs to create active oxygen radicals (e.g., O_2^- , OH^\cdot), which induce the degradation of organic dyes (MB).

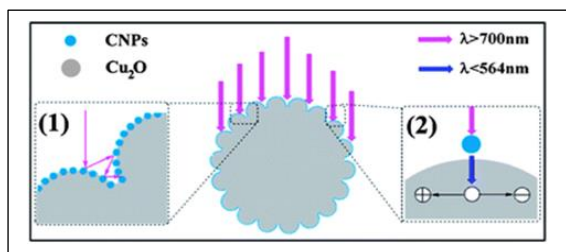


Figure 18. The schematic photocatalytic mechanism for the CQDs/ Cu_2O composite under (N)IR light irradiation [164].

Pan. et al. [165] manufactured The CQDs modified granular SnO_2 nanotubes using a simple technical procedure in which SnO_2 nanotubes are distributed in CQDs solution and then dried at 80°C . It shows that the photocatalytic efficiency of these composites is greatly improved by the degradation of Rhodamine B under visible light irradiation. Furthermore, the remarkable granular, tube-shaped structure of the SnO_2 and the carbon dots' unusual up-converted photoluminescence activity is thought to be the main reasons for this improvement.

4.1.2 Metal-organic framework (MOFs) as photocatalyst for removing organic dyes:

The photodegradation of organic molecules by MOFs has been thoroughly studied in recent years. Generally, three important steps are involved for the degradation of dyes by MOF-photocatalysts; (1) the photosensitizers of the organic bonds are activated to create an electron-hole pair, (2) the electrons and holes are migrated to the reactive centers, (3) the reduction and oxidation of the half-reactions induce redox equivalents (electrons and holes) in the photocatalytic center [166, 167]. MOFs' major advantage for dye degradation compared to regular inorganic semiconductors is the outstanding optical properties adjustment by modifying or manipulating the organic linker and the metal centers [168, 169].

Lan et al. [170] studied the efficiency of synthesized cluster-based organic-inorganic hybrid material ($[\text{NiL}_4\text{V}^{\text{IV}}\text{W}^{\text{VI}}_{10}\text{W}^{\text{V}}_2\text{O}_{40}(\text{V}^{\text{IV}}\text{O})_2]$, L is 1,4-bis(imidazol-1-yl) methyl)benzene) on photodegradation of MB and RhB. The results showed that the photodegradation rate curve is almost linear, achieving about 32% and 29.3% per hour under UV

light. The authors hypothesized that VO^{2+} groups would enhance photocatalytic activity. Furthermore, it is highly stable and easily separated from the photocatalytic system for reuse again. Du et al. [171] have used MIL-(M) (where M = Al, Cr, Fe) for the photodegradation of MB dye. Photocatalytic tests were performed under ultraviolet and visible light irradiation. The result showed that MIL-53(Fe) achieved similar activity with TiO_2 in the MB dye's photodegradation under both UV and visible irradiation. The catalyst has achieved a photodegradation efficacy 11% and 3% under UV- and light irradiation, respectively. The low efficiency is attributed to fast electron-hole recombination.

Wang et al. [172] report the synthesis of UiO-66(Ti) through the post-grafting method. UiO-66(Ti) nanocomposites' photocatalytic performance was evaluated in removing MB dye under sunlight irradiation. The authors reported that MB's adsorption during the first half-hour was very high and began to decrease until an hour elapsed, achieving 46.3%. The titanium content affects the adsorption of MB dye, where increasing titanium content leads to increasing adsorption of the dye. Like the UiO-66containing titanium, it was the only one that gave light activity (compared to the UiO-66), achieving 82% photodegradation.

Ai et al. [173] studied MIL-53 (Fe) efficiency in activating hydrogen peroxide to enhance RhB dye's photolysis under visible light irradiation. The hydrogen peroxide achieved 17.6% removal of the dye, while the dye was completely removed in the presence of the MIL-53 (Fe) photocatalyst. The authors considered this enhanced catalytic activity to be arising from synergistic effects by combining MIL-53 (Fe) and H_2O_2 under visible light irradiation, facilitating the generation of hydroxyl radicals.

Zhang et al. [174] described $\text{Fe}_3\text{O}_4@\text{C}/\text{Cu}$ and $\text{Fe}_3\text{O}_4@\text{CuO}$ composites. The composite was prepared via direct calcination of magnetic $\text{Fe}_3\text{O}_4@\text{HKUST-1}$ under air and N_2 conditions and used as a photocatalyst to degrade MB dye. The $\text{Fe}_3\text{O}_4@\text{C}/\text{Cu}$ photocatalyst showed low activity in the absence of H_2O_2 , and the photocatalytic activity increased with the addition of hydrogen peroxide. It was reported that Cu NPs have a low Fermi level, which can be a good receiver for electrons, which facilitates electron transfer from Fe_3O_4 under visible light irradiation. Consequently, the probability of photoinduced holes to a recombined excited electron is decreased.

The g- C_3N_4 coated MIL-100(Fe) composite through chemical protonation of g- C_3N_4 powder, and sol dip-coating was synthesized by Huang et al. [175] and used for the photocatalytic degradation of RhB

and MB. The results indicate that the protonated $g\text{-C}_3\text{N}_4$ was equally coated with good interaction along the MIL-100(Fe) framework, and the composite kept the advantages of the two parent materials. The composite exhibits an improved photocatalytic efficiency for RhB and MB degradation under visible light irradiation compared to the parent materials. The $g\text{-C}_3\text{N}_4$ achieved 53.4% removal for MB, and the protonated $g\text{-C}_3\text{N}_4$ gives lower removal, while that MIL-100(Fe) exhibited no photodegradation activity for MB. Despite the weak catalytic activity, MIL-100(Fe) achieved an adsorption rate of 85% of MB. The protonated $g\text{-C}_3\text{N}_4$ materials showed the advantage of photodegradation of MB dye compared with virgin MIL-100(Fe) as it acts as an adsorbent for MB only.

According to technology derives from coating MOFs with MOFs, Abdelhameed et al. [176] were post-synthetically a modified metal-organic framework (MIL-125-NH₂) with various ratios of zeolitic imidazolate framework-67 (ZIF-67). In visible light irradiation, the nanocomposite was used for selective photocatalytic removal of nitro-phenols. In comparison to P25, the nanocomposite demonstrated high photocatalytic activity as well as selectivity. Mahmoodi et al. [177] synthesized three metal-organic frameworks (Materials of Institut Lavoisier: MILs-100 (Fe)) as porous nanomaterials using FeCl₃, Fe(NO₃)₃ and Fe₂(SO₄)₃ and denoted as MIL-100-1, MIL-100-2, and MIL-100-3, respectively. The photocatalytic dye degradation potential of the synthesized metal-organic frameworks was investigated using Basic Blue 41 (BB41) as a model dye. The nanomaterials decolorized BB41, according to the findings. MIL-100-1 had a higher photocatalytic capacity, according to the results. For three cycles, MIL-100's catalytic performance did not decrease significantly. It can be inferred that MILs-100 (Fe) synthesized could be used as an alternate catalyst for photocatalytic decolorization of colored wastewater.

Abdelhameed et al.[178] reduced The band gap of NH₂-MIL-125 by a suitable post-synthetic modification of the nanochannels using conventional organic chemistry methods. NH₂-MIL-125 is a highly porous metal-organic framework (MOF) with a band gap lying within the ultraviolet region at about 2.6 eV. Post-synthetic change accompanied by Cr (III) complexation increases the photocatalytic behavior of NH₂-MIL-125 in methylene blue degradation under visible light. The last metal ion transfers the absorption from the UV to the visible area of light (band gap 2.21 eV). The photogenerated holes move from the MOF valence band to the Cr (III) valence band, promote hole and electron separation and increase the recovery time. Furthermore, doping with Ag nanoparticles, which are formed by the reduction of Ag⁺ with the

acetylacetonate pendant groups, significantly improves the MOF's photocatalytic activity (the resulting MOF band gap is 2.09 eV) (Figure 19). The nanoparticles Ag could be able to accept photogenerated electrons from the MOF, thereby preventing recombination of electron-hole. In photocatalytic conditions, all Cr and Ag-bearing materials are stable. These results open up new ways in which photocatalytic MOFs can be improved.

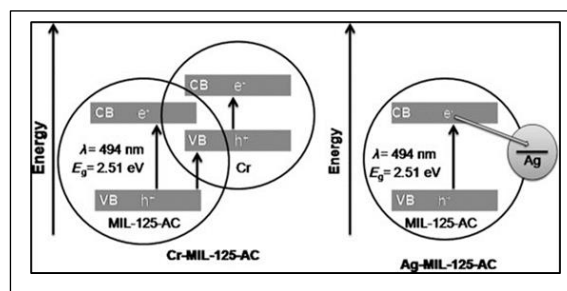


Figure 19. Schematic illustrations of the charge separation in Cr-MIL-125-AC (left) and the possible role of silver nanoparticles in trapping the photogenerated electrons (right) [178].

5. Summary and perspective

Organic mineral frameworks are easy to control their morphology by selecting the appropriate organic compound. They have a large surface area, controlled pore size, and good optical properties to be exploited in water treatment. The metal-organic framework's effectiveness is due to the promotion of the separation of electron-hole pairs and the suppression of the charge's recombination. These photocatalysis studies provide reliable and valuable principles for designing a highly effective photocatalyst from organic mineral frameworks and facilitating green chemistry and clean energy development.

MOFs have been effectively used for photocatalytic degradation of a large variety of organic pollutants in water. The dye degradation performance of MOF-based materials is strongly influenced by the optical absorption and charge separation efficiency properties, as well as the number of catalytic sites, which are connected to the central metals, the MOF structures, the intensity of conjugation, the coordinated atmosphere, and the steric hindrance around the active metal centers. Metal-based MOFs can be photo-excited directly to generate electrons and holes. The electrons produced by photo (e^-) would then be absorbed by oxygen molecules, resulting in superoxide radicals ($\cdot\text{O-O}\cdot$). Because of their good oxidizing potential, photogenerated (h^+) in the HOMO orbital can instantly oxidize organic molecules and can also react with water molecules to form hydroxyl radicals ($\cdot\text{OH}$). The reactive transit species (e.g., $\cdot\text{O}_2$

and •OH) used in dye photodegradation. Thus, adsorption with photocatalytic degradation under sunlight irradiation is a novel concept because it provides a comprehensive solution to pollutant removal from wastewater and safe remediation through environmentally benign organisms. MOFs and their composites seem to be suitable for these purposes.

Carbon dots as a new type of carbon-based fluorescent material have sparked in many publications. Various breakthroughs were documented, from basic photophysical properties to potential applications as photocatalysts. The positive role that carbon dots play in the charge transfer mechanism is very good, and it could be exploited to develop carbon dots-based photocatalysts. The means for preparing carbon dots and the proposed mechanism for photodegradation of some water-polluting organic dyes are also discussed briefly in this review. Looking at future carbon dot projections could play an important role in addressing environmental water pollution issues. But there is a need for a deeper understanding of surface activity relationships in carbon point-based systems, which is also highlighted in this review.

References

- [1] L. Rast W, Freshwater Storehouses and Mirrors of Human Activities, United Nations World Water Assessment Programme Programme Office for Global Water Assessment Division of Water Sciences, UNESCO, (2009) 1-4
- [2] T. Munir, D.M. Hussain, S. Naseem, Water Pollution-A Menace of Freshwater Biodiversity: A Review, JOURNAL OF ENTOMOLOGY AND ZOOLOGY STUDIES 4(4) (2016) 578-580.
- [3] M. AG, E.S. AM, S. MS, CURRENT SITUATION OF WATER POLLUTION AND ITS EFFECT ON AQUATIC LIFE IN EGYPT, Egyptian Journal of Occupational Medicine 37(1) (2013) 95-115.
- [4] A.M. Atta, I.F. Nassar, H.M. Bedawy, Unsaturated polyester resins based on rosin maleic anhydride adduct as corrosion protections of steel, Reactive and Functional Polymers 67(7) (2007) 617-626.
- [5] A.K. Dwivedi, RESEARCHES IN WATER POLLUTION: A REVIEW, International Research Journal of Natural and Applied Sciences 4(1) (2017).
- [6] R.P. Schwarzenbach, T. Egli, T.B. Hofstetter, U. von Gunten, B. Wehrli, Global Water Pollution and Human Health, Annual Review of Environment and Resources 35(1) (2010) 109-136.
- [7] Q. Zhou, Chemical Pollution and Transport of Organic Dyes in Water-Soil-Crop Systems of the Chinese Coast, Bulletin of Environmental Contamination and Toxicology 66(6) (2001) 0784-0793.
- [8] N.N. Mahapatra, Textile dyes, Woodhead Publishing India Pvt. Ltd (2016).
- [9] M.M. Hassan, C.M. Carr, A critical review on recent advancements of the removal of reactive dyes from dyehouse effluent by ion-exchange adsorbents, Chemosphere 209 (2018) 201-219.
- [10] M.A. Hassaan, A.E. Nemr, Health and Environmental Impacts of Dyes: Mini Review, American Journal of Environmental Science and Engineering 1(3) (2017) 64-67.
- [11] S. Khan, A. Malik, Toxicity evaluation of textile effluents and role of native soil bacterium in biodegradation of a textile dye, Environmental science and pollution research international 25(5) (2018) 4446-4458.
- [12] B. Lellis, C.Z. Fávaro-Polonio, J.A. Pamphile, J.C. Polonio, Effects of textile dyes on health and the environment and bioremediation potential of living organisms, Biotechnology Research and Innovation 3(2) (2019) 275-290.
- [13] M.E. Karim, K. Dhar, M.T. Hossain, Decolorization of Textile Reactive Dyes by Bacterial Monoculture and Consortium Screened from Textile Dyeing Effluent, Journal, genetic engineering & biotechnology 16(2) (2018) 375-380.
- [14] I. Safarik, L. Ptackova, M. Safarikova, ADSORPTION OF DYES ON MAGNETICALLY LABELED BAKER'S YEAST CELLS, European Cells and Materials 3(2) (2002) 52-55.
- [15] A.A. Aboul-Enein, F.S. Soliman, M.A. Betiha, Co-production of hydrogen and carbon nanomaterials using NiCu/SBA15 catalysts by pyrolysis of a wax by-product: Effect of Ni-Cu loading on the catalytic activity, International Journal of Hydrogen Energy 44(59) (2019) 31104-31120.
- [16] M.S. Mostafa, C. Lan, M.A. Betiha, R. Zhang, Y. Gao, G. Ge, Enhanced infrared-induced water oxidation by one-pot synthesized CoTi-Nanorods as highly infrared responsive photocatalyst, Journal of Power Sources 464 (2020).
- [17] H.M.A. Hassan, M.A. Betiha, S.K. Mohamed, E.A. El-Sharkawy, E.A. Ahmed, Stable and recyclable MIL-101(Cr)-Ionic liquid based hybrid nanomaterials as heterogeneous catalyst, Journal of Molecular Liquids 236 (2017) 385-394.
- [18] A.A. AlKahlaway, M.A. Betiha, D. Aman, A.M. Rabie, Facial synthesis of ferric molybdate (Fe₂(MoO₄)₃) nanoparticle and its efficiency for biodiesel synthesis via oleic acid esterification, Environmental Technology and Innovation 22 (2021).
- [19] M.R. Sayed, M.R. Abukhadra, S. Abdelkader Ahmed, M. Shaban, U. Javed, M.A. Betiha, J.J. Shim, A.M. Rabie, Synthesis of advanced MgAl-LDH based geopolymer as a potential catalyst in the conversion of waste sunflower oil into biodiesel: Response surface studies, Fuel 282 (2020).
- [20] M.A. Betiha, N.A. Negm, E.M. El-Sayed, M.S. Mostafa, M.F. Menoufy, Capability of synthesized sulfonated aromatic cross-linked polymer covalently bonded montmorillonite framework in productivity process of biodiesel, Journal of Cleaner Production 261 (2020).
- [21] M. Shaban, R. Hosny, A.M. Rabie, J.J. Shim, S.A. Ahmed, M.A. Betiha, N.A. Negm, Zinc aluminate nanoparticles: Preparation, characterization and application as efficient and economic catalyst in transformation of waste cooking oil into biodiesel, Journal of Molecular Liquids 302 (2020).
- [22] N.A. Negm, M.A. Betiha, M.S. Alhumaimess, H.M.A. Hassan, A.M. Rabie, Clean transesterification process for biodiesel production using heterogeneous polymer-

- heteropoly acid nanocatalyst, *Journal of Cleaner Production* 238 (2019).
- [23] M. Alhumaimess, O. Aldosari, H. Alshammari, M.M. Kamel, M.A. Betiha, H.M.A. Hassan, Ionic liquid green synthesis of CeO₂ nanorods and nano-cubes: Investigation of the shape dependent on catalytic performance, *Journal of Molecular Liquids* 279 (2019) 649-656.
- [24] H.M.A. Hassan, M.A. Betiha, R.F.M. Elshaarawy, E.A. Ahmed, Facile tailoring of hierarchical mesoporous AISBA-15 by ionic liquid and their applications in heterogeneous catalysis, *Journal of Porous Materials* 25(1) (2018) 63-73.
- [25] H.M.A. Hassan, M.A. Betiha, S.K. Mohamed, E.A. El-Sharkawy, E.A. Ahmed, Salen- Zr(IV) complex grafted into amine-tagged MIL-101(Cr) as a robust multifunctional catalyst for biodiesel production and organic transformation reactions, *Applied Surface Science* 412 (2017) 394-404.
- [26] M.A. Betiha, T. Mahmoud, A.M. Al-Sabagh, Effects of 4-vinylbenzyl trioctylphosphonium- bentonite containing poly(octadecylacrylate-co-1-vinyldodecanoate) pour point depressants on the cold flow characteristics of waxy crude oil, *Fuel* 282 (2020).
- [27] T. Mahmoud, M.A. Betiha, Poly(octadecyl acrylate- co-vinyl neodecanoate)/Oleic Acid-Modified Nano-graphene Oxide as a Pour Point Depressant and an Enhancer of Waxy Oil Transportation, *Energy and Fuels* (2021).
- [28] M.M. Abdelhamid, S.A. Rizk, M.A. Betiha, S.M. Desouky, A.M. Alsabagh, Improving heavy oil recovery, part (I): Synthesis and surface activity evaluation of some novel organometallic surfactants based on salen-M complexes, *RSC Advances* 11(3) (2021) 1750-1761.
- [29] H.E. Ahmed, M.A. Betiha, M. El-Dardir, M.F. Hussein, N.A. Negm, High-performance rheology modifiers and fluid loss of starch-bentonite system based mud fluids: Experimental and optimization study, *Egyptian Journal of Chemistry* 64(4) (2021) 1653-1664.
- [30] M.A. Betiha, M.M. Dardir, H. Abuseda, N.A. Negm, H.E. Ahmed, Improving the performance of water-based drilling fluid using amino acid-modified graphene oxide nanocomposite as a promising additive, *Egyptian Journal of Chemistry* 64(4) (2021) 1799-1806.
- [31] M.A. Betiha, S.B. El-Henawy, A.M. Al-Sabagh, N.A. Negm, T. Mahmoud, Experimental evaluation of cationic-Schiff base surfactants based on 5-chloromethyl salicylaldehyde for improving crude oil recovery and bactericide, *Journal of Molecular Liquids* 316 (2020).
- [32] M.A. Betiha, A.E. Elmetwally, A.M. Al-Sabagh, T. Mahmoud, Catalytic Aquathermolysis for Altering the Rheology of Asphaltic Crude Oil Using Ionic Liquid Modified Magnetic MWCNT, *Energy and Fuels* 34(9) (2020) 11353-11364.
- [33] M.A. Betiha, G.G. Mohamed, N.A. Negm, M.F. Hussein, H.E. Ahmed, Fabrication of ionic liquid-cellulose-silica hydrogels with appropriate thermal stability and good salt tolerance as potential drilling fluid, *Arabian Journal of Chemistry* 13(7) (2020) 6201-6220.
- [34] M.A. Betiha, A.M. Rabie, A.M. Elfadly, F.Z. Yehia, Microwave assisted synthesis of a VO_x-modified disordered mesoporous silica for ethylbenzene dehydrogenation in presence of CO₂, *Microporous and Mesoporous Materials* 222 (2016) 44-54.
- [35] A.A. Abdelrahman, M.A. Betiha, A.M. Rabie, H.S. Ahmed, M.F. Elshahat, Removal of refractory Organo-sulfur compounds using an efficient and recyclable {Mo132} nanoball supported graphene oxide, *Journal of Molecular Liquids* 252 (2018) 121-132.
- [36] A.S. Mansour, M.A. Betiha, Z.A. Alrowaili, S.A. Abubshait, N.A. Negm, A facile synthetic approach and optical properties of AuNPs/CdSe tetrapod and AuNPs/CdSe@rGO nanocomposites, *Journal of Molecular Liquids* 293 (2019).
- [37] A. Amiri, R. Tayebee, A. Abdar, F. Narenji Sani, Synthesis of a zinc-based metal-organic framework with histamine as an organic linker for the dispersive solid-phase extraction of organophosphorus pesticides in water and fruit juice samples, *Journal of Chromatography A* 1597 (2019) 39-45.
- [38] Y.-Z. Chen, R. Zhang, L. Jiao, H.-L. Jiang, Metal-organic framework-derived porous materials for catalysis, *Coordination Chemistry Reviews* 362 (2018) 1-23.
- [39] M.A. Betiha, Y.M. Moustafa, M.F. El-Shahat, E. Rafik, Polyvinylpyrrolidone-Aminopropyl-SBA-15 schiff Base hybrid for efficient removal of divalent heavy metal cations from wastewater, *Journal of hazardous materials* 397 (2020) 122675.
- [40] M.A. Betiha, Y.M. Moustafa, A.S. Mansour, E. Rafik, M.F. El-Shahat, Nontoxic polyvinylpyrrolidone-propylmethacrylate-silica nanocomposite for efficient adsorption of lead, copper, and nickel cations from contaminated wastewater, *Journal of Molecular Liquids* 314 (2020) 113656.
- [41] A.M. Rabie, H.M. Abd El-Salam, M.A. Betiha, H.H. El-Maghrabi, D. Aman, Mercury removal from aqueous solution via functionalized mesoporous silica nanoparticles with the amine compound, *Egyptian Journal of Petroleum* 28(3) (2019) 289-296.
- [42] S.K. Mohamed, A.A. Ibrahim, A.A. Mousa, M.A. Betiha, E.A. El-Sharkawy, H.M.A. Hassan, Facile fabrication of ordered mesoporous Bi/Ti-MCM-41 nanocomposites for visible light-driven photocatalytic degradation of methylene blue and CO oxidation, *Separation and Purification Technology* 195 (2018) 174-183.
- [43] H.M.A. Hassan, M.A. Betiha, R.F.M. Elshaarawy, M. Samy El-Shall, Promotion effect of palladium on Co₃O₄ incorporated within mesoporous MCM-41 silica for CO Oxidation, *Applied Surface Science* 402 (2017) 99-107.
- [44] H.M.A. Hassan, M.A. Betiha, A.E.R.S. Khder, M. Mostafa, M. Gallab, Hafnium pentachloride ionic liquid for isomorphic and postsynthesis of HfKIT-6 mesoporous silica: catalytic performances of Pd/SO₂-/HfKIT-6, *Journal of Porous Materials* 23(5) (2016) 1339-1351.
- [45] M.S. Abdel Salam, M.A. Betiha, S.A. Shaban, A.M. Elsabagh, R.M. Abd El-Aal, F.Y. El kady, Synthesis and characterization of MCM-41-supported nano zirconia catalysts, *Egyptian Journal of Petroleum* 24(1) (2015) 49-57.
- [46] H.M.A. Hassan, E.M. Saad, M.S. Soltan, M.A. Betiha, I.S. Butler, S.I. Mostafa, A palladium(II) 4-hydroxysalicylidene Schiff-base complex anchored on functionalized MCM-41: An efficient heterogeneous catalyst for the epoxidation of olefins, *Applied Catalysis A: General* 488 (2014) 148-159.
- [47] A.M. Elfadly, A.M. Badawi, F.Z. Yehia, Y.A. Mohamed, M.A. Betiha, A.M. Rabie, Selective nano alumina supported vanadium oxide catalysts for oxidative dehydrogenation of ethylbenzene to styrene using CO₂ as soft oxidant, *Egyptian Journal of Petroleum* 22(3) (2013) 373-380.
- [48] M.A. Betiha, H.M.A. Hassan, A.M. Al-Sabagh, A.E.R.S. Khder, E.A. Ahmed, Direct synthesis and the morphological control of highly ordered mesoporous AISBA-15 using urea-tetrachloroaluminate as a novel

- aluminum source, *Journal of Materials Chemistry* 22(34) (2012) 17551-17559.
- [49] M.A. Betiha, S.A. Mahmoud, M.F. Menoufy, A.M. Al-Sabagh, One-pot template synthesis of Ti–Al-containing mesoporous silicas and their application as potential photocatalytic degradation of chlorophenols, *Applied Catalysis B: Environmental* 107(3) (2011) 316-326.
- [50] M.A. Betiha, H.M.A. Hassan, E.A. El-Sharkawy, A.M. Al-Sabagh, M.F. Menoufy, H.E.M. Abdelmoniem, A new approach to polymer-supported phosphotungstic acid: Application for glycerol acetylation using robust sustainable acidic heterogeneous-homogenous catalyst, *Applied Catalysis B: Environmental* 182 (2016) 15-25.
- [51] B.T. Yonemoto, G.S. Hutchings, F. Jiao, A General Synthetic Approach for Ordered Mesoporous Metal Sulfides, *Journal of the American Chemical Society* 136(25) (2014) 8895-8898.
- [52] S.-L. Xiao, Y.-H. Li, P.-J. Ma, G.-H. Cui, Synthesis and characterizations of two bis(benzimidazole)-based cobaltous coordination polymers with high adsorption capacity for congo red dye, *Inorganic Chemistry Communications* 37 (2013) 54-58.
- [53] T.M. McDonald, J.A. Mason, X. Kong, E.D. Bloch, D. Gygi, A. Dani, V. Crocellà, F. Giordanino, S.O. Odoh, W.S. Drisdell, B. Vlasisavljevich, A.L. Dzubak, R. Poloni, S.K. Schnell, N. Planas, K. Lee, T. Pascal, L.F. Wan, D. Prendergast, J.B. Neaton, B. Smit, J.B. Kortright, L. Gagliardi, S. Bordiga, J.A. Reimer, J.R. Long, Cooperative insertion of CO₂ in diamine-appended metal-organic frameworks, *Nature* 519(7543) (2015) 303-308.
- [54] T. Zhang, W. Lin, Metal-organic frameworks for artificial photosynthesis and photocatalysis, *Chemical Society reviews* 43(16) (2014) 5982-5993.
- [55] H. Furukawa, N. Ko, Y.B. Go, N. Aratani, S.B. Choi, E. Choi, A.Ö. Yazaydin, R.Q. Snurr, M. O’Keeffe, J. Kim, O.M. Yaghi, Ultrahigh Porosity in Metal-Organic Frameworks, *Science* 329 (2010) 424-428.
- [56] L.J. Murray, M. Dinca, J.R. Long, Hydrogen storage in metal-organic frameworks, *Chemical Society reviews* 38(5) (2009) 1294-314.
- [57] Y.Q. Lan, H.L. Jiang, S.L. Li, Q. Xu, Mesoporous metal-organic frameworks with size-tunable cages: selective CO₂ uptake, encapsulation of Ln(3)(+) cations for luminescence, and column-chromatographic dye separation, *Advanced materials* 23(43) (2011) 5015-20.
- [58] L. Tang, Y.P. Fu, N. Cui, J.J. Wang, X.Y. Hou, X. Wang, A MOF based on a lead(II) 2-oxido-6-methylpyridine-4-carboxylate network, *Zeitschrift für Naturforschung B* 75(4) (2020) 365-369.
- [59] S. Dhaka, R. Kumar, A. Deep, M.B. Kurade, S.-W. Ji, B.-H. Jeon, Metal-organic frameworks (MOFs) for the removal of emerging contaminants from aquatic environments, *Coordination Chemistry Reviews* 380 (2019) 330-352.
- [60] a. Bourrelly, P.L. Llewellyn, C. Serre, F. Millange, T. Loiseau, G. Férey, Different Adsorption Behaviors of Methane and Carbon Dioxide in the Isotypic Nanoporous Metal Terephthalates MIL-53 and MIL-47, *J. AM. CHEM. SOC.* 127 (2005) 13519-13521.
- [61] R. Zou, R. Zhong, S. Han, H. Xu, A.K. Burrell, N. Henson, J.L. Cape, D.D. Hickmott, T.V. Timofeeva, T.E. Larson, Y. Zhao, A Porous Metal-Organic Replica of r-PbO₂ for Capture of Nerve Agent Surrogate, *J. AM. CHEM. SOC.* 132 (2010) 17996-17999.
- [62] B. Chen, N.W. Ockwig, A.R. Millward, D.S. Contreras, O.M. Yaghi, High H₂ adsorption in a microporous metal-organic framework with open metal sites, *Angewandte Chemie* 44(30) (2005) 4745-9.
- [63] L. Ma, C. Abney, W. Lin, Enantioselective catalysis with homochiral metal-organic frameworks, *Chemical Society reviews* 38(5) (2009) 1248-56.
- [64] L. Carlucci, G. Ciani, S. Maggini, D.M. Proserpio, M. Visconti, Heterometallic modular metal-organic 3D frameworks assembled via new tris-beta-diketonate metalloligands: nanoporous materials for anion exchange and scaffolding of selected anionic guests, *Chemistry* 16(41) (2010) 12328-41.
- [65] O.M. Yaghi, G. Li, Mutually Interpenetrating Sheets and Channels in the Extended Structure of [Cu(4,4'-bpy)Cl], *Angewandte Chemie International Edition in English* 34(2) (1995) 207-209.
- [66] Y. Xu, H. Wang, X. Li, X. Zeng, Z. Du, J. Cao, W. Jiang, Metal-organic framework for the extraction and detection of pesticides from food commodities, *Comprehensive Reviews in Food Science and Food Safety* 20(1) (2021) 1009-1035.
- [67] P.Z. Moghadam, A. Li, S.B. Wiggin, A. Tao, A.G.P. Maloney, P.A. Wood, S.C. Ward, D. Fairen-Jimenez, Development of a Cambridge Structural Database Subset: A Collection of Metal-Organic Frameworks for Past, Present, and Future, *Chemistry of Materials* 29(7) (2017) 2618-2625.
- [68] H.R. Abid, Z.H. Rada, J. Shang, S. Wang, Synthesis, characterization, and CO₂ adsorption of three metal-organic frameworks (MOFs): MIL-53, MIL-96, and amino-MIL-53, *Polyhedron* 120 (2016) 103-111.
- [69] J.H. Cavka, S. Jakobsen, U. Olsbye, N. Guillou, C. Lamberti, S. Bordiga, K.P. Lillerud, A New Zirconium Inorganic Building Brick Forming Metal Organic Frameworks with Exceptional Stability, *Journal of the American Chemical Society* 130(42) (2008) 13850-13851.
- [70] C. Xin, H. Zhan, X. Huang, H. Li, N. Zhao, F. Xiao, W. Wei, Y. Sun, Effect of various alkaline agents on the size and morphology of nano-sized HKUST-1 for CO₂ adsorption, *RSC Advances* 5(35) (2015) 27901-27911.
- [71] S. Hausdorf, F. Baitalow, T. Böhle, D. Rafaja, F.O.R.L. Mertens, Main-Group and Transition-Element IRMOF Homologues, *Journal of the American Chemical Society* 132(32) (2010) 10978-10981.
- [72] F. Şahin, B. Topuz, H. Kalıpçılar, Synthesis of ZIF-7, ZIF-8, ZIF-67 and ZIF-L from recycled mother liquors, *Microporous and Mesoporous Materials* 261 (2018) 259-267.
- [73] R. Banerjee, A. Phan, B. Wang, C. Knobler, H. Furukawa, M. O’Keeffe, O.M. Yaghi, High-Throughput Synthesis of Zeolitic Imidazolate Frameworks and Application to CO₂ Capture, *science vision* 319 (2008) 939-942.
- [74] A. PHAN, C.J. DOONAN, F.J. URIBE-ROMO, C.B. KNOBLER, M. O’KEEFFE, O.M. YAGHI, Synthesis, Structure, and Carbon Dioxide Capture Properties of Zeolitic Imidazolate Frameworks, *Accounts of chemical research* 43(1) (2010) 58-67.
- [75] W.J. Rieter, K.M.L. Taylor, W. Lin, Surface Modification and Functionalization of Nanoscale Metal-Organic Frameworks for Controlled Release and Luminescence Sensing, *J. AM. CHEM. SOC.* 129 (2007) 9852-9853.

- [76] H.-L. Jiang, B. Liu, T. Akita, M. Haruta, H. Sakurai, Q. Xu, Au@ZIF-8: CO Oxidation over Gold Nanoparticles Deposited to Metal-Organic Framework, *J. AM. CHEM. SOC.* 131(32) (2009) 11302–11303.
- [77] C.Y. Sun, C. Qin, X.L. Wang, G.S. Yang, K.Z. Shao, Y.Q. Lan, Z.M. Su, P. Huang, C.G. Wang, E.B. Wang, Zeolitic Imidazolate framework-8 as efficient pH-sensitive drug delivery vehicle, *Dalton transactions* 41(23) (2012) 6906-9.
- [78] X. Sun, Y. Lei, Fluorescent carbon dots and their sensing applications, *TrAC Trends in Analytical Chemistry* 89 (2017) 163-180.
- [79] P.G. Luo, S. Sahu, S.-T. Yang, S.K. Sonkar, J. Wang, H. Wang, G.E. LeCroy, L. Cao, Y.-P. Sun, Carbon “quantum” dots for optical bioimaging, *Journal of Materials Chemistry B* 1(16) (2013) 2116–2127.
- [80] I. Ahmed, B.N. Bhadra, H.J. Lee, S.H. Jung, Metal-organic framework-derived carbons: Preparation from ZIF-8 and application in the adsorptive removal of sulfamethoxazole from water, *Catalysis Today* 301 (2018) 90-97.
- [81] I. Costas-Mora, V. Romero, I. Lavilla, C. Bendicho, In Situ Building of a Nanoprobe Based on Fluorescent Carbon Dots for Methylmercury Detection, *Analytical Chemistry* 86(9) (2014) 4536-4543.
- [82] X. Xu, R. Ray, Y. Gu, H.J. Ploehn, L. Gearheart, K. Raker, W.A. Scrivens, Electrophoretic Analysis and Purification of Fluorescent Single-Walled Carbon Nanotube Fragments, *J. AM. CHEM. SOC.* 126 (2004) 12736-12737.
- [83] Y.-P. Sun, B. Zhou, Y. Lin, W. Wang, K.A.S. Fernando, P. Pathak, M.J. Meziani, B.A. Harruff, X. Wang, H. Wang, P.G. Luo, H. Yang, M.E. Kose, B. Chen, L.M. Veca, S.-Y. Xie, Quantum-Sized Carbon Dots for Bright and Colorful Photoluminescence, *J. AM. CHEM. SOC.* 128 (2006) 7756-7757.
- [84] L. Zheng, Y. Chi, Y. Dong, J. Lin, B. Wang, Electrochemiluminescence of Water-Soluble Carbon Nanocrystals Released Electrochemically from Graphite, *J. AM. CHEM. SOC.* 131 (2009) 4564–4565.
- [85] R. Liu, D. Wu, S. Liu, K. Koynov, W. Knoll, Q. Li, An aqueous route to multicolor photoluminescent carbon dots using silica spheres as carriers, *Angewandte Chemie* 48(25) (2009) 4598-601.
- [86] W. Beaton, R. Bertolacini, Resid hydroprocessing at Amoco, *Catalysis Reviews* 33(3-4) (1991) 281-317.
- [87] H. Liu, T. Ye, C. Mao, Fluorescent carbon nanoparticles derived from candle soot, *Angewandte Chemie* 46(34) (2007) 6473-5.
- [88] C. Long, Z. Jiang, J. Shangguan, T. Qing, P. Zhang, B. Feng, Applications of carbon dots in environmental pollution control: A review, *Chemical Engineering Journal* 406 (2021) 126848.
- [89] Y.-P. Sun, B. Zhou, Y. Lin, W. Wang, K.A.S. Fernando, P. Pathak, M.J. Meziani, B.A. Harruff, X. Wang, H. Wang, P.G. Luo, H. Yang, M.E. Kose, B. Chen, L.M. Veca, S.-Y. Xie, Quantum-Sized Carbon Dots for Bright and Colorful Photoluminescence, *Journal of the American Chemical Society* 128(24) (2006) 7756-7757.
- [90] S.-L. Hu, K.-Y. Niu, J. Sun, J. Yang, N.-Q. Zhao, X.-W. Du, One-step synthesis of fluorescent carbon nanoparticles by laser irradiation, *Journal of Materials Chemistry* 19(4) (2009) 484-488.
- [91] X. Wang, L. Cao, F. Lu, M.J. Meziani, H. Li, G. Qi, B. Zhou, B.A. Harruff, F. Kermarrec, Y.-P. Sun, Photoinduced electron transfers with carbon dots, *Chemical Communications* (25) (2009) 3774-3776.
- [92] L. Cao, X. Wang, M.J. Meziani, F. Lu, H. Wang, P.G. Luo, Y. Lin, B.A. Harruff, L.M. Veca, D. Murray, S.-Y. Xie, Y.-P. Sun, Carbon Dots for Multiphoton Bioimaging, *Journal of the American Chemical Society* 129(37) (2007) 11318-11319.
- [93] L. Xiao, H. Sun, Novel properties and applications of carbon nanodots, *Nanoscale Horizons* 3(6) (2018) 565-597.
- [94] J. Zhou, C. Booker, R. Li, X. Zhou, T.-K. Sham, X. Sun, Z. Ding, An Electrochemical Avenue to Blue Luminescent Nanocrystals from Multiwalled Carbon Nanotubes (MWCNTs), *Journal of the American Chemical Society* 129(4) (2007) 744-745.
- [95] H. Li, X. He, Z. Kang, H. Huang, Y. Liu, J. Liu, S. Lian, C.H.A. Tsang, X. Yang, S.-T. Lee, Water-Soluble Fluorescent Carbon Quantum Dots and Photocatalyst Design, *Angewandte Chemie International Edition* 49(26) (2010) 4430-4434.
- [96] Y. Li, Y. Hu, Y. Zhao, G. Shi, L. Deng, Y. Hou, L. Qu, An Electrochemical Avenue to Green-Luminescent Graphene Quantum Dots as Potential Electron-Acceptors for Photovoltaics, *Advanced Materials* 23(6) (2011) 776-780.
- [97] Q.-L. Zhao, Z.-L. Zhang, B.-H. Huang, J. Peng, M. Zhang, D.-W. Pang, Facile preparation of low cytotoxicity fluorescent carbon nanocrystals by electrooxidation of graphite, *Chemical Communications* (41) (2008) 5116-5118.
- [98] H. Liu, T. Ye, C. Mao, Fluorescent Carbon Nanoparticles Derived from Candle Soot, *Angewandte Chemie International Edition* 46(34) (2007) 6473-6475.
- [99] J. Peng, W. Gao, B.K. Gupta, Z. Liu, R. Romero-Aburto, L. Ge, L. Song, L.B. Alemany, X. Zhan, G. Gao, S.A. Vithayathil, B.A. Kaiparettu, A.A. Martí, T. Hayashi, J.-J. Zhu, P.M. Ajayan, Graphene Quantum Dots Derived from Carbon Fibers, *Nano Letters* 12(2) (2012) 844-849.
- [100] R. Ye, C. Xiang, J. Lin, Z. Peng, K. Huang, Z. Yan, N.P. Cook, E.L.G. Samuel, C.-C. Hwang, G. Ruan, G. Ceriotti, A.-R.O. Raji, A.A. Martí, J.M. Tour, Coal as an abundant source of graphene quantum dots, *Nature Communications* 4(1) (2013) 2943.
- [101] A.B. Bourlinos, A. Stassinopoulos, D. Anglos, R. Zboril, M. Karakassides, E.P. Giannelis, Surface Functionalized Carbogenic Quantum Dots, *Small* 4(4) (2008) 455-458.
- [102] M.J. Krysmann, A. Kelarakis, P. Dallas, E.P. Giannelis, Formation Mechanism of Carbogenic Nanoparticles with Dual Photoluminescence Emission, *Journal of the American Chemical Society* 134(2) (2012) 747-750.
- [103] F. Wang, M. Kreiter, B. He, S. Pang, C.-y. Liu, Synthesis of direct white-light emitting carbogenic quantum dots, *Chemical Communications* 46(19) (2010) 3309-3311.
- [104] X. Guo, C.-F. Wang, Z.-Y. Yu, L. Chen, S. Chen, Facile access to versatile fluorescent carbon dots toward light-emitting diodes, *Chemical Communications* 48(21) (2012) 2692-2694.
- [105] S.-S. Liu, C.-F. Wang, C.-X. Li, J. Wang, L.-H. Mao, S. Chen, Hair-derived carbon dots toward versatile multidimensional fluorescent materials, *Journal of Materials Chemistry C* 2(32) (2014) 6477-6483.
- [106] Z.-C. Yang, M. Wang, A.M. Yong, S.Y. Wong, X.-H. Zhang, H. Tan, A.Y. Chang, X. Li, J. Wang, Intrinsically fluorescent carbon dots with tunable emission derived from hydrothermal treatment of glucose in the presence of

- monopotassium phosphate, *Chemical Communications* 47(42) (2011) 11615-11617.
- [107] S. Sahu, B. Behera, T.K. Maiti, S. Mohapatra, Simple one-step synthesis of highly luminescent carbon dots from orange juice: application as excellent bio-imaging agents, *Chemical Communications* 48(70) (2012) 8835-8837.
- [108] L. Wang, H.S. Zhou, Green Synthesis of Luminescent Nitrogen-Doped Carbon Dots from Milk and Its Imaging Application, *Analytical Chemistry* 86(18) (2014) 8902-8905.
- [109] P.-C. Hsu, H.-T. Chang, Synthesis of high-quality carbon nanodots from hydrophilic compounds: role of functional groups, *Chemical Communications* 48(33) (2012) 3984-3986.
- [110] D. Pan, J. Zhang, Z. Li, M. Wu, Hydrothermal Route for Cutting Graphene Sheets into Blue-Luminescent Graphene Quantum Dots, *Advanced Materials* 22(6) (2010) 734-738.
- [111] K. Holá, M. Sudolská, S. Kalytchuk, D. Nachtigallová, A.L. Rogach, M. Otyepka, R. Zbořil, Graphitic Nitrogen Triggers Red Fluorescence in Carbon Dots, *ACS Nano* 11(12) (2017) 12402-12410.
- [112] G. Ren, M. Tang, F. Chai, H. Wu, One-Pot Synthesis of Highly Fluorescent Carbon Dots from Spinach and Multipurpose Applications, *European Journal of Inorganic Chemistry* 2018(2) (2018) 153-158.
- [113] H. Zhu, X. Wang, Y. Li, Z. Wang, F. Yang, X. Yang, Microwave synthesis of fluorescent carbon nanoparticles with electrochemiluminescence properties, *Chemical Communications* (34) (2009) 5118-5120.
- [114] X. Zhai, P. Zhang, C. Liu, T. Bai, W. Li, L. Dai, W. Liu, Highly luminescent carbon nanodots by microwave-assisted pyrolysis, *Chemical Communications* 48(64) (2012) 7955-7957.
- [115] S. Chandra, P. Das, S. Bag, D. Laha, P. Pramanik, Synthesis, functionalization and bioimaging applications of highly fluorescent carbon nanoparticles, *Nanoscale* 3(4) (2011) 1533-1540.
- [116] S. Qu, X. Wang, Q. Lu, X. Liu, L. Wang, A biocompatible fluorescent ink based on water-soluble luminescent carbon nanodots, *Angewandte Chemie International Edition* 124(49) (2012) 12381-12384.
- [117] R. Liu, D. Wu, S. Liu, K. Koynov, W. Knoll, Q. Li, An aqueous route to multicolor photoluminescent carbon dots using silica spheres as carriers, *Angewandte Chemie International Edition* 48(25) (2009) 4598-4601.
- [118] B. Wang, Y. Mu, H. Yin, Z. Yang, Y. Shi, J. Li, Formation and origin of multicenter photoluminescence in zeolite-based carbogenic nanodots, *Nanoscale* 10(22) (2018) 10650-10656.
- [119] A.B. Bourlinos, A. Stassinopoulos, D. Anglos, R. Zboril, V. Georgakilas, E.P. Giannelis, Photoluminescent Carbogenic Dots, *Chemistry of Materials* 20(14) (2008) 4539-4541.
- [120] S.N. Baker, G.A. Baker, Luminescent carbon nanodots: emergent nanolights, *Angewandte Chemie* 49(38) (2010) 6726-44.
- [121] K.O. Boakye-Yiadom, S. Kesse, Y. Opoku-Damoah, M.S. Filli, M. Aquib, M.M.B. Joelle, M.A. Farooq, R. Mavlyanova, F. Raza, R. Bavi, B. Wang, Carbon dots: Applications in bioimaging and theranostics, *International Journal of Pharmaceutics* 564 (2019) 308-317.
- [122] J. Zong, Y. Zhu, X. Yang, J. Shen, C. Li, Synthesis of photoluminescent carbogenic dots using mesoporous silica spheres as nanoreactors, *Chemical communications* 47(2) (2011) 764-6.
- [123] I.Y. Goryacheva, A.V. Sapelkin, G.B. Sukhorukov, Carbon nanodots: Mechanisms of photoluminescence and principles of application, *TrAC Trends in Analytical Chemistry* 90 (2017) 27-37.
- [124] N.A. Negm, M.T.H.A. Kana, S.A. Abubshait, M.A. Betiha, Effectuality of chitosan biopolymer and its derivatives during antioxidant applications, *International Journal of Biological Macromolecules* 164 (2020) 1342-1369.
- [125] N.A. Negm, H.A. Abubshait, S.A. Abubshait, M.T.H. Abou Kana, E.A. Mohamed, M.M. Betiha, Performance of chitosan polymer as platform during sensors fabrication and sensing applications, *International Journal of Biological Macromolecules* 165 (2020) 402-435.
- [126] Z.G. Gu, D.J. Li, C. Zheng, Y. Kang, C. Wöll, J. Zhang, MOF-Templated Synthesis of Ultrasmall Photoluminescent Carbon-Nanodot Arrays for Optical Applications, *Angewandte Chemie International Edition* 56(24) (2017) 6853-6858.
- [127] Z.-G. Gu, D.-J. Li, C. Zheng, Y. Kang, C. Wöll, J. Zhang, MOF-Templated Synthesis of Ultrasmall Photoluminescent Carbon-Nanodot Arrays for Optical Applications, *Angewandte Chemie International Edition* 56(24) (2017) 6853-6858.
- [128] H. Xu, S. Zhou, L. Xiao, H. Wang, S. Li, Q. Yuan, Fabrication of a nitrogen-doped graphene quantum dot from MOF-derived porous carbon and its application for highly selective fluorescence detection of Fe³⁺, *Journal of Materials Chemistry C* 3(2) (2015) 291-297.
- [129] Y. Yang, D. Wu, S. Han, P. Hu, R. Liu, Bottom-up fabrication of photoluminescent carbon dots with uniform morphology via a soft-hard template approach, *Chemical Communications* 49(43) (2013) 4920-4922.
- [130] E. Pajootan, M. Arami, N.M. Mahmoodi, Binary system dye removal by electrocoagulation from synthetic and real colored wastewaters, *Journal of the Taiwan Institute of Chemical Engineers* 43(2) (2012) 282-290.
- [131] B. Kayan, B. Gozmen, M. Demirel, A.M. Gizir, Degradation of acid red 97 dye in aqueous medium using wet oxidation and electro-Fenton techniques, *Journal of hazardous materials* 177(1-3) (2010) 95-102.
- [132] M.Y. Nassar, M.M. Moustafa, M.M. Taha, Hydrothermal tuning of the morphology and particle size of hydrozincite nanoparticles using different counterions to produce nanosized ZnO as an efficient adsorbent for textile dye removal, *RSC Adv.* 6(48) (2016) 42180-42195.
- [133] M.Y. Nassar, I.S. Ahmed, I. Samir, A novel synthetic route for magnesium aluminate (MgAl₂O₄) nanoparticles using sol-gel auto combustion method and their photocatalytic properties, *Spectrochimica acta. Part A, Molecular and biomolecular spectroscopy* 131 (2014) 329-34.
- [134] M. Djenouhat, F. Bendebane, L. Bahloul, M.E.H. Samar, F. Ismail, Optimization of methylene blue removal by stable emulsified liquid membrane using Plackett-Burman and Box-Behnken designs of experiments, *Royal Society open science* 5(2) (2018) 171220.
- [135] Q. Wu, W.-T. Li, W.-H. Yu, Y. Li, A.-M. Li, Removal of fluorescent dissolved organic matter in biologically treated textile wastewater by ozonation-biological aerated filter, *Journal of the Taiwan Institute of Chemical Engineers* 59 (2016) 359-364.

- [136] A.B. Fradj, S.B. Hamouda, H. Ouni, R. Lafi, L. Gzara, A. Hafiane, Removal of methylene blue from aqueous solutions by poly(acrylic acid) and poly(ammonium acrylate) assisted ultrafiltration, *Separation and Purification Technology* 133 (2014) 76-81.
- [137] A. Mohammadzadeh, M. Ramezani, A.M. Ghaedi, Synthesis and characterization of Fe₂O₃-ZnO-ZnFe₂O₄/carbon nanocomposite and its application to removal of bromophenol blue dye using ultrasonic assisted method: Optimization by response surface methodology and genetic algorithm, *Journal of the Taiwan Institute of Chemical Engineers* 59 (2016) 275-284.
- [138] N. Serpone, A.V. Emeline, Semiconductor Photocatalysis - Past, Present, and Future Outlook, *The journal of physical chemistry letters* 3(5) (2012) 673-7.
- [139] N. Serpone, A.V. Emeline, S. Horikoshi, V.N. Kuznetsov, V.K. Ryabchuk, On the genesis of heterogeneous photocatalysis: a brief historical perspective in the period 1910 to the mid-1980s, *Photochemical & photobiological sciences : Official journal of the European Photochemistry Association and the European Society for Photobiology* 11(7) (2012) 1121-50.
- [140] J.H. Golbeck, *Photosystem I: the light-driven plastocyanin: ferredoxin oxidoreductase*, Springer Science & Business Media 2007.
- [141] D.G. Nocera, The artificial leaf, *Accounts of chemical research* 45(5) (2012) 767-776.
- [142] P. Boddy, Oxygen evolution on semiconducting TiO₂, *Journal of The Electrochemical Society* 115(2) (1968) 199.
- [143] A. Fujishima, K. Honda, Electrochemical Photolysis of Water at a Semiconductor Electrode, *Nature* 238(5358) (1972) 37-38.
- [144] F.E. Osterloh, Photocatalysis versus photosynthesis: a sensitivity analysis of devices for solar energy conversion and chemical transformations, *ACS Energy Letters* 2(2) (2017) 445-453.
- [145] S. Chen, T. Takata, K. Domen, Particulate photocatalysts for overall water splitting, *Nature Reviews Materials* 2(10) (2017) 1-17.
- [146] X. Chang, T. Wang, J. Gong, CO₂ photo-reduction: insights into CO₂ activation and reaction on surfaces of photocatalysts, *Energy & Environmental Science* 9(7) (2016) 2177-2196.
- [147] J.A. Dean, *Solubilities of inorganic compounds and metal salts of organic acids in water at various temperatures*, Lange's Handbook of Chemistry (1999).
- [148] A.D. McNaught, A. Wilkinson, *Compendium of chemical terminology*, Blackwell Science Oxford 1997.
- [149] L. Zhang, X. Yuan, H. Wang, X. Chen, Z. Wu, Y. Liu, S. Gu, Q. Jiang, G. Zeng, Facile preparation of an Ag/AgVO₃/BiOCl composite and its enhanced photocatalytic behavior for methylene blue degradation, *RSC Advances* 5(119) (2015) 98184-98193.
- [150] Y.-P. Yuan, L.-S. Yin, S.-W. Cao, G.-S. Xu, C.-H. Li, C. Xue, Improving photocatalytic hydrogen production of metal-organic framework UiO-66 octahedrons by dye-sensitization, *Applied Catalysis B: Environmental* 168-169 (2015) 572-576.
- [151] X. He, K. Fang, X.-H. Guo, J. Han, X.-P. Lu, M.-X. Li, A homochiral Cu(I) coordination polymer based on achiral precursors and its photocatalytic properties, *Dalton transactions* 44(30) (2015) 13545-13549.
- [152] M.A. Nasalevich, M. Van Der Veen, F. Kapteijn, J. Gascon, Metal-organic frameworks as heterogeneous photocatalysts: Advantages and challenges, *CrystEngComm* 16(23) (2014) 4919-4926.
- [153] Y. Pi, X. Li, Q. Xia, J. Wu, Y. Li, J. Xiao, Z. Li, Adsorptive and photocatalytic removal of Persistent Organic Pollutants (POPs) in water by metal-organic frameworks (MOFs), *Chemical Engineering Journal* 337 (2018) 351-371.
- [154] M. Wen, K. Mori, Y. Kuwahara, T. An, H. Yamashita, Design of Single-Site Photocatalysts by Using Metal-Organic Frameworks as a Matrix, *Chemistry - An Asian Journal* 13(14) (2018) 1767-1779.
- [155] Z. Zhang, X. Li, B. Liu, Q. Zhao, G. Chen, Hexagonal microspindle of NH₂-MIL-101(Fe) metal-organic frameworks with visible-light-induced photocatalytic activity for the degradation of toluene, *RSC Advances* 6(6) (2016) 4289-4295.
- [156] X. Li, Z. Le, X. Chen, Z. Li, W. Wang, X. Liu, A. Wu, P. Xu, D. Zhang, Graphene oxide enhanced amine-functionalized titanium metal organic framework for visible-light-driven photocatalytic oxidation of gaseous pollutants, *Applied Catalysis B: Environmental* 236 (2018) 501-508.
- [157] Y. Lu, Y. Feng, F. Wang, X. Zou, Z.-F. Chen, P. Chen, H. Liu, Y. Su, Q. Zhang, G. Liu, Facile hydrothermal synthesis of carbon dots (CDs) doped ZnFe₂O₄/TiO₂ hybrid materials with high photocatalytic activity, *Journal of Photochemistry and Photobiology A: Chemistry* 353 (2018) 10-18.
- [158] H. Zhang, H. Huang, H. Ming, H. Li, L. Zhang, Y. Liu, Z. Kang, Carbon quantum dots/Ag₃PO₄ complex photocatalysts with enhanced photocatalytic activity and stability under visible light, *Journal of Materials Chemistry* 22(21) (2012) 10501-10506.
- [159] J. Zhang, X. Zhang, S. Dong, X. Zhou, S. Dong, N-doped carbon quantum dots/TiO₂ hybrid composites with enhanced visible light driven photocatalytic activity toward dye wastewater degradation and mechanism insight, *Journal of Photochemistry and Photobiology A: Chemistry* 325 (2016) 104-110.
- [160] R. Kannan, A.R. Kim, S.K. Eo, S.H. Kang, D.J. Yoo, Facile one-step synthesis of cerium oxide-carbon quantum dots/RGO nanohybrid catalyst and its enhanced photocatalytic activity, *Ceramics International* 43(3) (2017) 3072-3079.
- [161] P. Atkin, T. Daeneke, Y. Wang, B.J. Carey, K.J. Berean, R.M. Clark, J.Z. Ou, A. Trinchì, I.S. Cole, K. Kalantar-zadeh, 2D WS₂/carbon dot hybrids with enhanced photocatalytic activity, *Journal of Materials Chemistry A* 4(35) (2016) 13563-13571.
- [162] Z. Qu, J. Wang, J. Tang, X. Shu, X. Liu, Z. Zhang, J. Wang, Carbon quantum dots/KNbO₃ hybrid composites with enhanced visible-light driven photocatalytic activity toward dye waste-water degradation and hydrogen production, *Molecular Catalysis* 445 (2018) 1-11.
- [163] P. ReddyPrasad, E.B. Naidoo, Ultrasonic synthesis of high fluorescent C-dots and modified with CuWO₄ nanocomposite for effective photocatalytic activity, *Journal of Molecular Structure* 1098 (2015) 146-152.
- [164] H. Li, R. Liu, Y. Liu, H. Huang, H. Yu, H. Ming, S. Lian, S.-T. Lee, Z. Kang, Carbon quantum dots/Cu₂O composites with protruding nanostructures and their highly efficient (near) infrared photocatalytic behavior, *Journal of Materials Chemistry* 22(34) (2012) 17470-17475.
- [165] J. Pan, Y. Zhou, J. Cao, Y. Sheng, Y. Wu, C. Cui, C. Li, B. Feng, Fabrication of carbon quantum dots modified

- granular SnO₂ nanotubes for visible light photocatalysis, *Materials Letters* 170 (2016) 187-191.
- [166] C.-C. Wang, X.-D. Du, J. Li, X.-X. Guo, P. Wang, J. Zhang, Photocatalytic Cr(VI) reduction in metal-organic frameworks: A mini-review, *Applied Catalysis B: Environmental* 193 (2016) 198-216.
- [167] W.-T. Xu, L. Ma, F. Ke, F.-M. Peng, G.-S. Xu, Y.-H. Shen, J.-F. Zhu, L.-G. Qiu, Y.-P. Yuan, Metal-organic frameworks MIL-88A hexagonal microrods as a new photocatalyst for efficient decolorization of methylene blue dye, *Dalton transactions* 43(9) (2014) 3792-3798.
- [168] S. Bala, S. Bhattacharya, A. Goswami, A. Adhikary, S. Konar, R. Mondal, Designing Functional Metal-Organic Frameworks by Imparting a Hexanuclear Copper-Based Secondary Building Unit Specific Properties: Structural Correlation With Magnetic and Photocatalytic Activity, *Crystal Growth & Design* 14(12) (2014) 6391-6398.
- [169] J. Zhao, W.-W. Dong, Y.-P. Wu, Y.-N. Wang, C. Wang, D.-S. Li, Q.-C. Zhang, Two (3,6)-connected porous metal-organic frameworks based on linear trinuclear [Co₃(COO)₆] and paddlewheel dinuclear [Cu₂(COO)₄] SBUs: gas adsorption, photocatalytic behaviour, and magnetic properties, *Journal of Materials Chemistry A* 3(13) (2015) 6962-6969.
- [170] Q. Lan, Z.-M. Zhang, Y.-G. Li, Y. Lu, E.-B. Wang, Synthesis of a poly-pendant 1-D chain based on 'trans-vanadium' bicapped, Keggin-type vanadotungstate and its photocatalytic properties, *Dalton transactions* 43(43) (2014) 16265-16269.
- [171] J.-J. Du, Y.-P. Yuan, J.-X. Sun, F.-M. Peng, X. Jiang, L.-G. Qiu, A.-J. Xie, Y.-H. Shen, J.-F. Zhu, New photocatalysts based on MIL-53 metal-organic frameworks for the decolorization of methylene blue dye, *Journal of Hazardous Materials* 190(1) (2011) 945-951.
- [172] A. Wang, Y. Zhou, Z. Wang, M. Chen, L. Sun, X. Liu, Titanium incorporated with UiO-66(Zr)-type Metal-Organic Framework (MOF) for photocatalytic application, *RSC Advances* 6(5) (2016) 3671-3679.
- [173] L. Ai, C. Zhang, L. Li, J. Jiang, Iron terephthalate metal-organic framework: Revealing the effective activation of hydrogen peroxide for the degradation of organic dye under visible light irradiation, *Applied Catalysis B: Environmental* 148-149 (2014) 191-200.
- [174] Y.-F. Zhang, L.-G. Qiu, Y.-P. Yuan, Y.-J. Zhu, X. Jiang, J.-D. Xiao, Magnetic Fe₃O₄@C/Cu and Fe₃O₄@CuO core-shell composites constructed from MOF-based materials and their photocatalytic properties under visible light, *Applied Catalysis B: Environmental* 144 (2014) 863-869.
- [175] J. Huang, X. Zhang, H. Song, C. Chen, F. Han, C. Wen, Protonated graphitic carbon nitride coated metal-organic frameworks with enhanced visible-light photocatalytic activity for contaminants degradation, *Applied Surface Science* 441 (2018) 85-98.
- [176] R.M. Abdelhameed, M. El-Shahat, Fabrication of ZIF-67@MIL-125-NH₂ nanocomposite with enhanced visible light photoreduction activity, *Journal of Environmental Chemical Engineering* 7(3) (2019) 103194.
- [177] N.M. Mahmoodi, J. Abdi, M. Oveisi, M. Alinia Asli, M. Vossoughi, Metal-organic framework (MIL-100 (Fe)): Synthesis, detailed photocatalytic dye degradation ability in colored textile wastewater and recycling, *Materials Research Bulletin* 100 (2018) 357-366.
- [178] R.M. Abdelhameed, M.M.Q. Simões, A.M.S. Silva, J. Rocha, Enhanced Photocatalytic Activity of MIL-125 by Post-Synthetic Modification with Cr^{III} and Ag Nanoparticles, *Chemistry – A European Journal* 21(31) (2015) 11072-11081.